Environmental Modelling & Software 24 (2009) 341–358

Contents lists available at ScienceDirect

Environmental Modelling & Software

journal homepage: www.elsevier.com/locate/envsoft

Generalization of a statistical downscaling model to provide local climate change projections for Australia

B. Timbal*, E. Fernandez, Z. Li

Centre for Australian Weather and Climate Research, Bureau of Meteorology, P.O. Box 1289, Melbourne 3001, Australia

ARTICLE INFO

Article history:
Received 6 December 2007
Received in revised form 23 July 2008
Accepted 23 July 2008
Available online 25 September 2008

Keywords:
Statistical downscaling
Graphical user interface
Climate change projections
Australia
Validation

ABSTRACT

Climate change information required for impact studies is of a much finer spatial scale than climate models can directly provide. Statistical downscaling models (SDMs) are commonly used to fill this scale gap. SDMs are based on the view that the regional climate is conditioned by two factors: (1) the large-scale climatic state and (2) local physiographic features. An SDM based on an analogue approach has been developed within the Australian Bureau of Meteorology and applied to six regions covering the southern half of Australia. Six surface predictands (daily minimum and maximum temperature and dew-point temperature, daily total rainfall and pan evaporation) were modelled. The skill of the SDMs is evaluated by comparing reconstructed and observed series using a range of metrics: first two moments of the series, the ability to reproduce day-to-day and inter-annual variability, and long-term trends. Once optimised, the SDMs are applied to a selection of global climate models which contributed to the Intergovernmental Panel on Climate Change 4th assessment report released in 2007. A user-friendly graphical interface has been developed to facilitate dissemination of the SDM results and provides a range of options for users to obtain tailored information. Once the projections are calculated for the places of interest, graphical outputs are displayed and can be downloaded jointly with the underlying data, allowing the user to use the data in their own application.

1. Introduction

Global climate models (GCMs) have resolutions of hundreds of kilometres, whilst regional climate models (RCMs) may be as fine as tens of kilometres. However, impact assessment applications often require point specific climate projections in order to capture fine-scale climate variations, particularly in regions with complex topography, coastal or island locations, and in areas of highly heterogeneous land-cover. Therefore a gap exists between what climate models can predict about future climate change and the information relevant for environmental studies. Statistical Downscaling Models (SDMs) are commonly used to fill this gap.

SDMs are based on the premise that the regional climate is conditioned by two factors: the large-scale climatic state and local physiographic features. From this perspective, regional or local climate information is derived by first determining a statistical model which relates large-scale climate variables (or "predictors") to regional and local variables (or "predictands"). The large-scale output of a GCM simulation is then fed into this statistical model to estimate the corresponding local and regional climate characteristics. There have been numerous applications of SDMs both in Australia and elsewhere. According to the latest IPCC assessment: "*Research on SDM has shown an extensive growth in application, and includes an increased availability of generic tools for the impact community*" (p. 920, chapter 11, IPCC 4th assessment, Christensen et al., 2007).

The Australian Bureau of Meteorology (BoM) has developed an SDM using the idea of a meteorological analogue (Timbal and McAvaney, 2001). This is one example of a more general type of SDM based on weather classification methods in which predictands are chosen by matching previous (i.e. analogous situations) to the current weather-state. The method was originally designed for weather forecasting applications (Lorenz, 1969) but was abandoned due to its limited success and lack of suitable analogues for systems with large degrees of freedom (Van Den Dool, 1994). The popularity of the method has recently increased with the availability of longer time-series datasets, following the completion of several reanalysis projects and the recognition that the dimension of the search space (i.e. the spatial domain and number of predictors) must be suitably restricted when identifying analogues. Even so, the analogue method still performs poorly when the pool of training observations is limited and/or the number of classifying predictors is large.

The BoM SDM was first developed for daily temperature maximum and minimum (T_{min} and T_{max}) across the Murray–Darling basin (MDB) in Australia (Timbal and McAvaney, 2001). The

* Corresponding author.
E-mail address: b.timbal@bom.gov.au (B. Timbal).

1364-8152/$ – see front matter
doi:10.1016/j.envsoft.2008.07.007

choice of a single, best analogue is based on a closest neighbour using a simple Euclidean metric. The metric is applied to a single vector which comprises daily normalised anomalies of point values within an optimised geographical area for the selected predictors. The choice of the optimal combination of predictors and the geographical area are two key steps in the optimisation of the analogue model. The SDM was then extended to rainfall occurrences (Timbal et al., 2003) and amount (Timbal, 2004). During these applications, the technique was tested on other mid-latitude geographical areas in both Australia and Europe. More recently, the early work on temperature and rainfall was extended to the newly derived high-quality network data for the surface moisture related variables pan evaporation and dew-point temperature. Therefore the BoM SDM is currently applied to six surface predictands.

The ability of the SDM to reproduce a shift in the observed climate, a proxy for its ability to reproduce a shift in a future climate due to global warming, has been tested for the rainfall decline in the late 1960s in the Southwest of Western Australia (SWA, Timbal, 2004), and in the mid 1990s in the South East of Australia (SEA, Timbal and Jones, 2008). These studies demonstrated the ability of the statistical linkage to reproduce non-stationary climates. However this addresses only one of the several possible limitations often cited for SDM (Hewitson and Crane, 2006; Christensen et al., 2007). Users should be familiar with these issues and possible limitations in using downscaled outputs (see Timbal, 2006a, for the particular case of the SDM presented here) as well as being aware of the important benefits brought by SDMs compared with using Direct Model Outputs (DMOs). A more complete discussion of the advantages of the particular SDM described here is given in Timbal (2006b). In using downscaled projections it is also important to follow best practice as recommended by the IPCC (Wilby et al., 2004).

To facilitate access to downscaling projections across a broader user community, a graphical user interface (GUI) has been developed, which provides projections across the southern half of the Australian continent. The GUI is a web-based tool using a mix of static HTML (HyperText Markup Language) pages and dynamically generated pages. It provides users with access to projections for a series of surface predictands at point specific locations. The locations correspond to the stations included in the high-quality climate data network maintained by the National Climate Centre (NCC) of the BoM. This network forms the basis of our current understanding of long-term trends and variability of the Australian climate.

The GUI has been developed specifically to be used within Australia and is particularly directed at impact studies (e.g. agriculture, health, ecology and economy). The scope is limited to part of the Australian continent and the statistical model has been optimised therefore users can generate data without specific knowledge of the particular statistical downscaling methodology. It responds to a growing need for efficient delivery mechanisms of climate change information.

Currently most available tools rely on DMOs rather than downscaled projections: e.g. the Ozclim software (http://www.csiro.au/ozclim/home.do) developed by the CSIRO to provide regional projections across the Australian continent where various climate models' information are interpolated on a high resolution grid (Ricketts and Page, 2007); or the TETYN software (http://sourceforge.net/projects/tetyn/) which used global database of climate indices (Solymosi et al., 2008). Besides tool based on DMOs, a few attempts have been made to enhance the relevance of the climate information provided by on-line software for high resolution impact studies by downscaling climate change information. The first documented attempt was the UK-based SDSM (www.sdsm.org.uk), this is a general downscaling methodology that one can optimise and applied anywhere once the local data needed are provided (Wilby et al., 2002); Hessami et al. (2008) described a regional optimisation and application for Canada. More similar in scope and method to the tool described here is the UK-based Environment agency Rainfall and Weather Impacts Generator, EARWIG however relies on a weather generator type of downscaling (Kilsby et al., 2007) as does RainSim (Burton et al., 2008) while the BoM-GUI, described here, relies on a physically based downscaling method rather than a stochastic weather generator: namely meteorological analogues, similar to the k-nearest neighbour approach described by Bannayan and Hoogenboom (2008).

After presenting the dataset used in Section 2, results from the optimisation of the SDM are presented in Section 3 and the skill of the downscaling model is discussed in Section 4. Finally, the graphical user interface developed to disseminate the downscaled projections is briefly described in Section 5, with a case study showing GUI outputs in Section 6 before a final discussion in Section 7.

2. Data

The development and validation of the SDM were performed using the highest quality possible for both surface predictands and large-scale predictors in order to limit the impact of data quality on the statistical linkage being developed.

2.1. Predictors: reanalyses

Global reanalyses of the atmosphere were used for the large-scale predictors. Both the NCEP/NCAR reanalysis datasets (NNR) (available from 1948 to real-time) (Kalnay et al., 1996) and the European Centre ERA40 reanalysis datasets (available from 1957 to 2003) (Uppala et al., 2005) were tested. The impact of data quality on the SDM performance was carefully assessed. It was found that NNR from 1958 (i.e. not using the earlier decade from 1948 to 1957) provided the best results and are therefore used as the basis to search for analogues from the global climate models.

2.2. Predictands

For surface predictands, the best possible stations available for observed long-term climate purposes are the High-Quality (HQ) dataset assembled by the NCC of the BoM. Variables used were daily HQ temperature maximum and minimum (Trewin, 2001) and daily HQ rainfall amount (Lavery et al., 1992, 1997). Both records were extended to 2005 by the NCC. More recently, HQ dataset was developed for surface humidity (dew-point daily maximum and minimum: dT_{min} and dT_{max}) by Lucas (2006) for the period 1957–2003 and for surface pan evaporation (pE) (Jovanovic et al., 2008) for the period 1975–2003.

Following on the early work on temperature and rainfall, the SDM was optimised for the newly formed HQ networks. Therefore downscaled projections for six surface predictands can be obtained through the GUI. Analogues are found over the period for which both reanalyses and surface predictands were deemed suitable: 1958–2003 for all variables, except for pan evaporation between 1975 and 2003. These periods were used to perform the development validation and optimisation of the individual SDMs and they are also the periods over which the analogues are found when the SDM is applied to climate models.

2.3. Predictors: climate models

As part of the Intergovernmental Panel on Climate Change (IPCC) 4th assessment of climate change science released in 2007 (Solomon et al., 2007) a new set of global climate model experiments has been produced. This represents a major advance both for

the evaluation of models, and for the generation of climate projections. The open nature of output availability has resulted in this set of experiments being subjected to unprecedented levels of evaluation and analysis: the Coupled Model Intercomparison Project No. 3 (CMIP3). Model outputs were obtained from the IPCC Model Output website at http://www-pcmdi.llnl.gov/ipcc/info_for_analysts.php.

Up to 23 GCMs contributed to the CMIP3 dataset. However because the SDM relies on daily outputs for the predictors, which were not provided by every modelling group, only a subset of this database could be used (Table 1). GCMs are used if the modelling group provided daily data for both the simulation of the 20th century and for simulations of the 21st century under different emission scenarios. The models were ranked according to a measure of their sensitivity (ΔT, last column in Table 1), calculated using the global warming produced by the model using the A1B scenario when approximated by linear regression over the 21st century (CSIRO and BoM, 2007).

Up to six future emission scenarios were used by the modelling groups that contributed to the CMIP3 database. Each emission scenario leads to a different projected global warming range (Table 2). In order to reduce the amount of data used, only two scenarios for the 21st century have been downscaled: A2 and B1. The A2 scenario is based on a very heterogeneous world with continuously increasing population and a technologically fragmented economic development leading to one of the highest emission scenarios available. In contrast, in B1 the emphasis is on global solutions to economic, social and environmental sustainability, and B1 is one of the lowest emission scenarios available. A simulation of the 20th century was also used to complement the scenarios. Daily data are therefore available for three time slices for which daily model predictors were available and downscaled and can be accessed through the GUI: 40 years from 1961 to 2000 from the 20th century simulation and two 20 year periods ranging from 2046 to 2065 in the middle, and from 2081 to 2100 at the end, of the 21st century, using either the A2 or B1 scenarios.

3. Optimisation of the SDM

3.1. Regions of interest

In order to apply the BoM SDM to the entire non-tropical half of the Australian continent (south of 30°S), surface observations were gathered into six distinct *climate entities* (Fig. 1), roughly following the rotated Empirical Orthogonal Functions (EOFs) for rainfall suggested by Drosdowsky (1993): (1) the Southwest of Western Australia (SWA), south of a north boundary from Geraldton to Kalgoorlie (about 30°S) and west of a line from Kalgoorlie to Esperance (about 122°E), (2) the Nullarbor (NUL) region: a vast region from the SWA in the west and the Eyre peninsula in South Australia in the east (about 136°E) and from the coast to 30°S, (3) the Southwest of Eastern Australia (SEA): southwest of a line from Melbourne (38°S and 145°E) to Port Augusta (33°S and 138°E), (4) the southern half of the Murray–Darling Basin (SMD) south of 30°S in the north, limited in the west by SEA and in the east by the Great Dividing Range (GDR), (5) the South-East Coast (SEC): a coastal band east of the GDR from Wilson Promontory in Victoria (39°S and 146°E) in the south all the way along the coast up to the Queensland Border in the north (28°S) and (6) the island of Tasmania (TAS) including all the Bass Strait islands. A summary of the number of surface predictands available in each climatic region (Table 3) indicates that although less than half of the Australian continent is covered by these six climatic regions, together they cover a large proportion of the available HQ observation sites (between 79% for rainfall and 58% for pan evaporation). It underlines the fact that these regions are the most populated in Australia (and hence the relatively denser network of observations in particular for rainfall) and therefore the most important for human related activities (e.g. agriculture).

Table 1
Global climate models from the CMIP3 database to which the SDM is applied

Originating group	Country	Acronym	Grid size (km)	ΔT (°C)
CSIRO	Australia	CSIRO	~200	2.11
NASA/Goddard Institute for Space Studies	U.S.A.	GISSR	~400	2.12
Canadian Climate Centre	Canada	CCM	~300	2.47
Meteorological Research Institute	Japan	MRI	~300	2.52
Geophysical Fluid Dynamics Lab	U.S.A.	GFDL2	~300	2.53
Meteo-France	France	CNRM	~200	2.81
Geophysical Fluid Dynamics Lab	U.S.A.	GFDL1	~300	2.98
Institut Pierre Simon Laplace	France	IPSL	~300	3.19
Centre for Climate Research	Japan	MIROC	~300	3.35
Max Planck Institute for meteorology DKRZ	Germany	MPI	~200	3.69

The name and country of the originating group, the acronym used in the GUI and the approximate size of the model horizontal grid box are shown. Models are ranked according to a measure of their sensitivity (ΔT, last column) from the lowest climate sensitivity at the top.

Table 2
Mean global warming estimates for 2090–2099, relative to 1980–1999, for 6 emission scenarios, derived from Figure SPM-3 of the IPCC (2007) report

Scenario	Mean warming (°C)	Uncertainty range (°C)
B1	1.8	1.1–2.9
A1T	2.4	1.4–3.8
B2	2.4	1.4–3.8
A1B	2.8	1.7–4.4
A2	3.4	2.0–5.4
A1FI	4.0	2.4–6.4

3.2. The optimisation methodology

Each individual SDM (a total of 144: six predictands times six regions times the four calendar seasons – summer: DJF, autumn: MAM, winter: JJA and spring: SON) was optimised using a range of statistics covering the ability of the SDM to reproduce the first two moments of the observed Probability Density Function (PDF) of the series (mean and variance), the skill of the model in reproducing day-to-day variability and inter-annual variability, as well as long-term linear trends. The optimisation methodology was based on a subjective analysis of these various metrics. No attempt was made to develop an objective approach in order to allow for expert knowledge of the importance of the different predictors and their inter-dependence. Furthermore, it is generally not the case that a single combination of predictors gives superior results for all metrics used and hence a trade-off exists between the importance of the various predictors and their role. The optimisation was performed in two steps. First the best combination of predictors was determined, and then three additional parameters were optimised using the best combination of predictors (second step).

3.3. The choice of predictors

The predictors considered were chosen on the basis of previous experience while developing the BoM SDM (Timbal and McAvaney, 2001; Timbal et al., 2003; Timbal, 2004), evidence in the literature from other studies in similar areas (Charles et al., 1999, 2003) and the availability of variables in the CMIP3 database. In most cases, the predictors are low level atmospheric fields but in some instances large-scale rainfall or T_{max} or T_{min} from the GCMs are used as predictors for local rainfall or T_{max} or T_{min}. The optimum combination of predictors varies across regions, seasons and

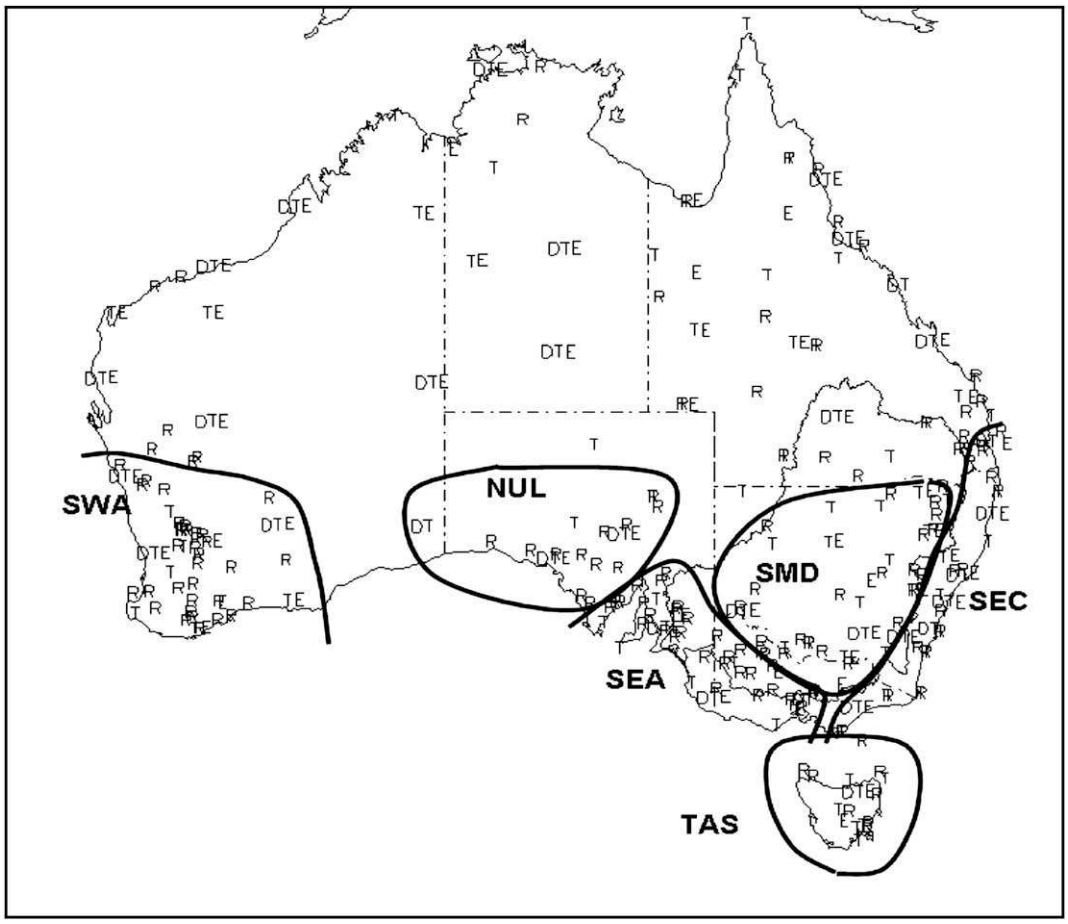

Fig. 1. Location of the high-quality networks across Australia for rainfall (R), temperature (T), dew-point temperature (D) and pan evaporation (E). The boundaries of the six areas of interest are overlayed: southwest of Australia (SWA), Nullarbor Plain (NUL), the southwest of eastern Australia (SEA), the southern part of the Murray–Darling Basin (SMD), the south-east coast (SEC) and Tasmania (TAS).

predictands (Table 4a and b). Statistics on the number of predictors used in optimised combination reveals that the optimal number is often three (apart from pan evaporation where most frequently only two predictors are used). When a different number of predictors are required for the optimum combination it is often less than three predictors apart from rainfall. The need for a large number of predictors for rainfall shows that it is a difficult predictand to capture from large-scale analogues. Not only does rainfall require a large number of atmospheric variables, it is the predictand for which skill scores are lowest (see details in the next section). There are only a few cases (for dT_{max} and dT_{min}) where no combinations of predictors were found to improve on the best performing single predictor.

Mean sea level pressure (MSLP) is the most frequently chosen predictor (Fig. 2, top left). It is used for all individual SDMs in the case of rainfall and T_{max} but is picked up far less often for pan evaporation. This feature, combined with the fact that the SDM shows overall low skill (discussed in the next section) for pan evaporation, suggests that MSLP is a critical predictor for a synoptically driven technique such as the analogue approach, and when it does not appear as a useful predictor none of the other available predictors can compensate for the lack of skill coming from MSLP.

Thermal predictors (Fig. 2, top right) are very important, especially for T_{max} and T_{min}. In general, T_{850} is the most important thermal predictor, although T_{min} is more important for dT_{min} and dT_{max}. Dew-point temperature, in most instances, has a weak diurnal cycle with maximum values in the early morning and maximal value in the afternoon (Lucas, 2006). Therefore, while the importance of T_{min} for dT_{max} is logical, its relevance for dT_{min} is less intuitive. A total percentage in excess of 100% means that in some cases more than one thermal predictor is used in the optimised combination. The additional predictor is usually T_{max} for T_{max} and T_{min} for T_{min}, a clear indication that in these cases lower tropospheric temperature alone is not a sufficient predictor. In these rare occurrences, with two very similar and highly correlated predictors being used, the risk of over-fitting the SDM exists. However, in these instances it was found that the gain in skill for the SDM warranted this choice. Finally, thermal predictors rarely matter for rainfall to reproduce current climate however, their importance in a future warmer world remains possible.

Moisture variables (Fig. 2, bottom left) are also important as predictors across the board with the notable exception of T_{max}. Specific humidity is almost always picked up apart from pan evaporation for which relative humidity is more skilful. Rainfall is often part of the optimised predictor's combination to downscale

Table 3
Number of high-quality stations available in each climatic region for the four types of predictand and the sum that the total of these stations in the six regions represent as a percentage of the respective entire high-quality network (last column)

Predictands	SWA	NUL	SEA	SMD	SEC	TAS	HQ network (%)
Temperature (T_{max} and T_{min})	9	5	11	15	16	7	70
Rainfall	34	12	31	24	11	8	79
Pan evaporation	7	2	5	9	7	3	58
Dew-point (dT_{max} and dT_{min})	3	3	3	2	7	1	60

Table 4a
Optimum combination of predictors for each calendar season and the six predictands in three regions: SWA, NUL and SEA

Predictands	Season	SWA	NUL	SEA
T_{max}	Summer	MSLP & T_{850} & V_{850}	MSLP & T_{850} & V_{850}	MSLP & T_{850}
	Autumn	MSLP & T_{850} & V_{850}	MSLP & T_{850} & V_{850}	MSLP & T_{max}
	Winter	MSLP & T_{850} & V_{850}	MSLP & T_{850} & U_{850}	MSLP & T_{850} & T_{max} & U_{850}
	Spring	MSLP & T_{850} & V_{850}	MSLP & T_{850} & V_{850}	MSLP & T_{850}
T_{min}	Summer	MSLP & T_{850} & Q_{850} & U_{850}	MSLP & T_{850} & Q_{850}	MSLP & T_{850}
	Autumn	MSLP & T_{850} & Q_{850} & U_{850}	T_{850} & Q_{850}	MSLP & T_{850} & Q_{850}
	Winter	MSLP & T_{850} & Q_{850}	MSLP & T_{850} & Q_{850} & U_{850}	MSLP & T_{850} & Q_{850}
	Spring	MSLP & T_{850} & Q_{850}	T_{850} & Q_{850}	MSLP & T_{850} & Q_{850}
Rain	Summer	MSLP & PRCP & Q_{850} & U_{850}	MSLP & PRCP & Q_{850} & U_{850}	MSLP & PRCP & T_{850}
	Autumn	MSLP & PRCP & Q_{850} & U_{850}	MSLP & T_{850} & Q_{850} & U_{850}	MSLP & T_{max} & Q_{850} & U_{850}
	Winter	MSLP & Q_{850} & U_{850}	MSLP & T_{850} & Q_{850} & U_{850}	MSLP & PRCP & V_{850}
	Spring	MSLP & Q_{850} & U_{850}	MSLP & Q_{850} & T_{850}	MSLP & PRCP
pE	Summer	MSLP & T_{max} & R_{925}	T_{850} & R_{925}	T_{max} & R_{925}
	Autumn	MSLP & T_{850} & R_{850}	T_{850} & R_{925}	T_{max} & R_{925}
	Winter	MSLP & T_{max} & R_{925}	T_{max} & R_{925}	T_{max} & R_{925}
	Spring	MSLP & T_{max} & R_{850}	T_{850} & R_{925}	T_{max} & R_{925}
dT_{max}	Summer	Q_{850} & T_{min}	MSLP & Q_{925} & T_{min}	MSLP & Q_{925}
	Autumn	MSLP & Q_{925} & T_{min}	MSLP & Q_{925}	MSLP & Q_{925} & T_{min} & V_{850}
	Winter	MSLP & Q_{850} & T_{min}	MSLP & Q_{925} & T_{min}	MSLP & Q_{925} & T_{min}
	Spring	Q_{850} & T_{850}	MSLP & Q_{925} & T_{min}	MSLP & Q_{925} & T_{min}
dT_{min}	Summer	Q_{925} & T_{min}	MSLP & Q_{925} & T_{min}	MSLP & Q_{925} & T_{min}
	Autumn	Q_{925} & T_{min}	MSLP & Q_{925}	MSLP & Q_{925} & T_{min}
	Winter	Q_{925} & T_{min}	MSLP & Q_{925} & T_{850}	MSLP & Q_{925} & T_{min}
	Spring	Q_{925} & T_{min}	Q_{925}	MSLP & Q_{925} & T_{min}

The predictors are defined as follows: MSLP is the Mean Sea Level Pressure; T_{max} and T_{min} are the 2 meter min and max temperature; PRCP is the total rainfall; Q is the specific humidity; R is the relative humidity; T is the temperature; U and V are the zonal and meridional wind components; and subscript numbers indicates the atmospheric level for the variable in hPa.

rainfall. As for temperature, there are instances (about 20% of the cases) where it is used in combination with another low level tropospheric moisture fields suggesting a possible over-fitting.

Finally, some measure of the air flow (either the zonal (u) or meridional (v) component of the wind) is often added to the optimised combination (Fig. 2, bottom right). The fact that it is an additional predictor to the de-facto combination of synoptic-thermal-moisture is evident from examining Tables 4a and b. It is most useful for rainfall and then T_{max}, and least useful for dew-point temperature and pan evaporation. The zonal component is the most frequently used.

It is worth remembering readers that the selection of the optimum combination of predictors is solely based on the past observed climate. The SDMs then rely on the hypothesis that the chosen predictors will capture the essence of the large-scale changes in a warmer future climate that will drive the local climate. This hypothesis has been investigated using discontinuities in our past climate record in specific cases discussed in Section 1, it will

Table 4b
Optimum combination of predictors for each calendar season and the six predictands in three regions: SMD, SEC and TAS

Predictands	Season	SMD	SEC	TAS
T_{max}	Summer	MSLP & T_{max}	MSLP & T_{max}	MSLP & T_{850} & T_{max} & U_{850}
	Autumn	MSLP & T_{max}	MSLP & T_{max}	MSLP & T_{850} & T_{max} & U_{850}
	Winter	MSLP & T_{850} & T_{max} & U_{850}	MSLP & T_{max}	MSLP & T_{850} & Q_{850} & U_{850}
	Spring	MSLP & T_{850} & U_{850}	MSLP & T_{850} & T_{max} & U_{850}	MSLP & T_{850} & T_{max} & U_{850}
T_{min}	Summer	T_{850} & Q_{850}	MSLP & T_{850} & Q_{850}	MSLP & T_{850} & Q_{850}
	Autumn	T_{850} & Q_{850}	MSLP & T_{850} & Q_{850}	MSLP & T_{850} & Q_{850}
	Winter	MSLP & T_{850} & Q_{850}	MSLP & T_{850} & T_{min} & U_{850}	MSLP & T_{850} & T_{min} & U_{850}
	Spring	MSLP & T_{850} & Q_{850}	MSLP & T_{850} & Q_{850}	MSLP & T_{850} & T_{min} & U_{850}
Rain	Summer	MSLP & PRCP & V_{850}	MSLP & T_{max} & Q_{850} & U_{850}	MSLP & Q_{850} & V_{850}
	Autumn	MSLP & PRCP & V_{850}	MSLP & PRCP & Q_{850} & U_{850}	MSLP & Q_{850} & V_{850}
	Winter	MSLP & PRCP & V_{850}	MSLP & PRCP & U_{850}	MSLP & PRCP & Q_{850} & U_{850}
	Spring	MSLP & PRCP & V_{850}	MSLP & PRCP & Q_{850} & U_{850}	MSLP & PRCP & Q_{850} & U_{850}
pE	Summer	T_{max} & R_{850}	T_{max} & R_{925}	MSLP & T_{850} & R_{925}
	Autumn	T_{max} & R_{850}	T_{max} & R_{925}	MSLP & T_{max}
	Winter	T_{max} & R_{925}	MSLP & T_{max} & R_{925}	MSLP & T_{max} & R_{925}
	Spring	T_{max} & R_{850}	T_{max} & R_{925} & U_{850}	MSLP & T_{max} & R_{925}
dT_{max}	Summer	MSLP & Q_{850} & T_{min} & V_{850}	MSLP & Q_{925} & T_{min}	MSLP & Q_{850}
	Autumn	MSLP & Q_{850} & T_{min} & V_{850}	MSLP & Q_{925} & T_{min}	MSLP & Q_{925}
	Winter	T_{min}	MSLP & Q_{925} & T_{min}	T_{min}
	Spring	MSLP & Q_{850}	MSLP & Q_{925} & T_{min}	MSLP & Q_{925} & T_{min}
dT_{min}	Summer	MSLP & Q_{850} & T_{850}	MSLP & Q_{925} & T_{min}	MSLP & Q_{850}
	Autumn	MSLP & Q_{850} & T_{min} & U_{850}	MSLP & Q_{925} & T_{min}	MSLP & Q_{925} & T_{min}
	Winter	MSLP & Q_{850} & T_{min} & V_{850}	MSLP & Q_{925} & T_{min}	MSLP & Q_{850} & T_{min}
	Spring	MSLP & Q_{850} & T_{850}	MSLP & Q_{925} & T_{min}	MSLP & Q_{925} & T_{min}

The predictors are defined as follows: MSLP is the Mean Sea Level Pressure; T_{max} and T_{min} are the 2 meter min and max temperature; PRCP is the total rainfall; Q is the specific humidity; R is the relative humidity; T is the temperature; U and V are the zonal and meridional wind components; and subscript numbers indicates the atmospheric level for the variable in hPa.

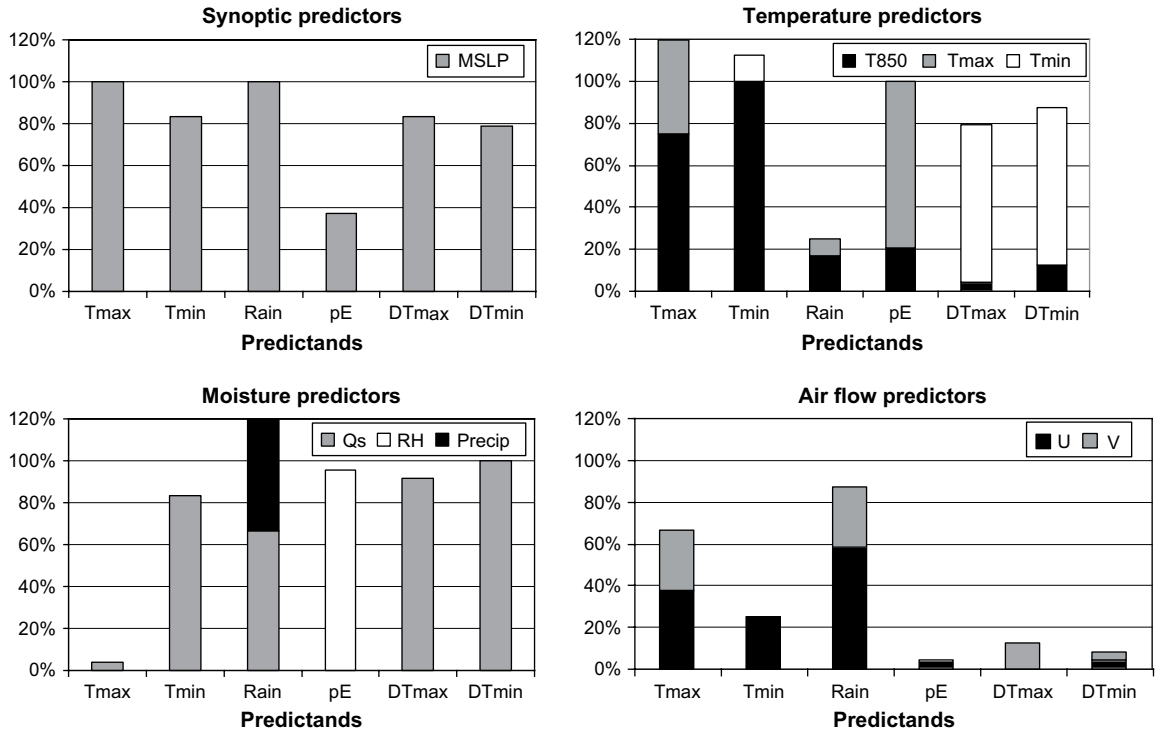

Fig. 2. Percentage of all existing SDMs, when a particular type of variable is part of the optimal combination of predictors: mean sea level pressure (top left), temperature predictors (top right), moisture predictors (bottom left) and air flow variables (bottom right) for the individual SDM separated according to the predictands being modelled: T_{max}, T_{min}, rainfall, pE, dT_{max} and dT_{min}. Each bar (i.e. 100%) is based on 24 cases: six regions times four seasons.

also be touched on during the evaluation of the skill of the model in particular the ability of the SDMs to reproduce observed trends.

3.4. Additional parameters

The BoM SDM includes a large number of tuneable parameters; however previous studies have shown that three parameters are particularly important (Timbal, 2004). Therefore the following three parameters were systematically explored as part of the extension of the technique across the Australian continent:

1. The size of the geographical domain used for the predictors (latitude and longitude). Only two domain sizes, chosen a-priori based on previous studies were tested (Fig. 3).
2. The calendar window from which analogues are found. Three periods were tested: 15, 30 and 60 days prior to and after the model date.
3. The way the daily anomalies are calculated using either three monthly values or a single seasonal average.

Overall statistics on the choice of the three additional parameters optimised for each individual SDM show some patterns worth commenting. The optimum size of the geographical domain that is used to search for analogues is most often the larger of the two sizes tested. There is a hint that the need to reduce the size of the geographical domain is seasonally dependent and use of the smaller domain is more frequent for the warmer seasons (42% of all SDMs in summer and 56% in autumn, compared to 33% and 28% in winter and spring). However, the most important factor appears to be the dependence on the region. It suggests that although the original two sizes tested for each region were chosen carefully based on rules derived from previous studies, there were cases (such as SWA) where the small domain was too small and hence seldom chosen (only 6% of the time); whereas in SMD, the small domain was chosen 50% of the time and between 20% and 30% in the other regions.

The choice between monthly or seasonal anomalies reveals a marked preference for using a single seasonal mean in particular for the transitional seasons (autumn 89% of all cases and spring 83%). This result was expected, as the underlying assumption behind using monthly mean is to reduce the non-stationarity across the months when calculating the anomalies, hence reducing the importance of the annual cycle when choosing an analogue. This result is particularly marked for temperature (94% of all SDMs for T_{max} and 92% for T_{min}) and less for rainfall (72%) as expected since the annual cycle is more pronounced for temperature than rainfall.

Finally, the calendar window (dT_{cal}) was tested (Fig. 4). This is the number of days before and after the calendar dates which are

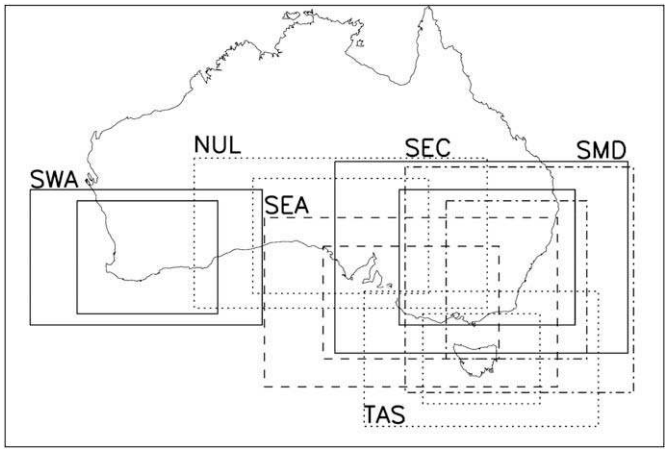

Fig. 3. Geographical domains (large and small) on which the predictors are used for the six areas of interest (SWA: plain, NUL: dotted, SEA: dashed, SMD: plain, SEC: dash-dotted and TAS: dotted).

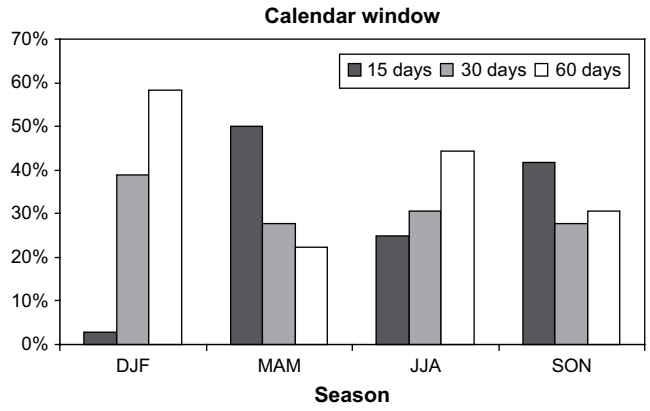

Fig. 4. Repartition between the optimal size of calendar windows (either 15, 30 or 60 days) in percentage of the total number of SDMs as a function of the season of the year (note: see main text for a full description of the calendar window).

used to find an analogue. For example, when searching for an analogue for the 1st of July:

- ✓ if $dT_{cal} = 15$ than analogues can only be chosen between the 16th of June and the 16th of July;
- ✓ if $dT_{cal} = 30$, analogue is chosen between the 1st of June and the 31st of July; and
- ✓ if $dT_{cal} = 60$, analogue is chosen between the 1st of June (this remains unchanged as analogues are only searched for within the same calendar season) and the 30th of August.

The limitation to search for an analogue only during the same calendar season is arbitrary but responds to a concern that the large-scale meteorological forcings of the local climate change during the year (as reflected in the optimum combination of predictors discussed earlier). Similarly, the size of the calendar window is used to force the choice of analogue during the same part of the season. However, a bigger value for the calendar window provides a potentially larger pool of analogues; hence the choice of the calendar window is a trade-off between these two effects. As expected, there is tendency to choose a smaller calendar window for the transient seasons (Spring and Autumn), when the underlying stationarity assumption is less true and a tendency to choose a large calendar window in winter, and in particular, in summer where the size of pool of analogue is most important.

4. Skill of the model

The SDM's skill was evaluated using a range of metrics on different time scales. First the ability of the technique to reproduce the observed probability distribution functions (PDFs) was evaluated by looking at the first two moments of the PDFs: the mean and the variance. The reproduction of the mean values for each of the predictands (Fig. 5) is very accurate. In each graph, points correspond to a single location for a single season with the observed mean value on the *x*-axis and the reconstructed mean along the *y*-axis. The number of points in each graph is equal to the total number of stations captured in one of the six climate regions times four seasons (between 480 for rainfall and 76 for dew-point temperature). For all predictands except rainfall, errors in the reproduction of the mean are negligible and there is no evidence that the SDMs have a bias toward either higher or lower values, including at the tails of the distribution (large or small observed values). However, in the case of rainfall, points are located below the diagonal, indicating a clear bias toward drier values for reconstructed series (between 15% in winter and 25% in summer).

Similarly results are shown for the reproduction of the standard deviation (Fig. 6). Clearly, the technique has a tendency to underestimate the observed variance: points are aligned below the diagonal for all variables. This is a known problem for regression-based statistical downscaling methods (Von Storch, 1999) and although the analogue approach is less affected, it appears to be an issue as well. This variance underestimation is relatively small. In the case of temperature (min and max), it is of the order of 5–10%, with the largest underestimations in winter. It is of the same magnitude for pan evaporation where the largest underestimation is in summer. The magnitude of the underestimation is slightly more for dew-point temperature, around 10% for dT_{max} and between 10% and 15% for dT_{min}. The underestimation of the variance for rainfall is larger than for the other variables: it varies between 20% in winter and up to 40% in summer.

For all variables, but rainfall as daily values are not normally distributed, the underestimation of the variance does not have a flow-on effect on the reproduction of the mean. In the case of rainfall on the other hand, the reproduction of the mean is dependent on the ability of the technique to reproduce the observed variance and results in the dry bias noted earlier (Fig. 5c).

For this reason, Timbal et al. (2006) introduced a correction factor to adjust the reconstructed rainfall series and enhance the variance and improve the reproduction of the mean. The rationale for the applied correction is that the analogue reconstructed rainfall is affected by the size of the pool of analogues which becomes smaller in the case of rare large rainfall events. Therefore, the error in finding the best matching analogue increases and the chances are that the best analogue found would describe more frequent but less intense rainfall events thus underestimating the rainfall in the reconstructed series. This problem exists across the range of climate used: from very dry (less than 20 mm per season to very wet up to 500 mm per season). Across the range of climates, it is assumed that the size of the pool depends on the ratio of rain days over dry days. It was decided that a very simple factor should be applied to limit some of the danger linked to artificially inflating the variance when using downscaling techniques (Von Storch, 1999). The following single factor was used, which only depends on the availability of dry and wet days to find a suitable analogue:

$$C_{factor} = 1. + 0.10 \times \frac{N_{dry}}{N_{wet}} \text{ and } C_{factor} \leq 1.5$$

where N_{dry} and N_{wet} are the numbers of dry and wet (>0.3 mm) days observed for the season at an individual location. These numbers are station and season dependent. They are calculated on the available observations from which analogues are drawn and are therefore independent of the series being reconstructed. These ratios are equally applicable when developing the downscaling model (and hence evaluating their impact) or when downscaling climate simulations. The impact of the inflation factor is clear (Fig. 7). It has dramatically reduced the variance bias and lead to an unbias reproduction of the mean (as for other predictands) and unbiased reproduction of the variance (which is not the case for the other uncorrected reconstructed predictands).

Besides the ability of the technique to reproduce the observed shape of the PDFs as defined by the first two moments of the series, it is important to ensure that the technique is skilful in reproducing day-to-day variability that is driven by large-scale synoptic changes. A random choice of analogue may reproduce perfectly the observed mean and variance but may not be a skilful model. The Pearson correlation between daily observed and reconstructed series was calculated separately per region, per season and for each predictand. Each number is an average across all observations available in each region (Fig. 8). The results show a contrast between predictands; the SDM appears more successful for T_{max},

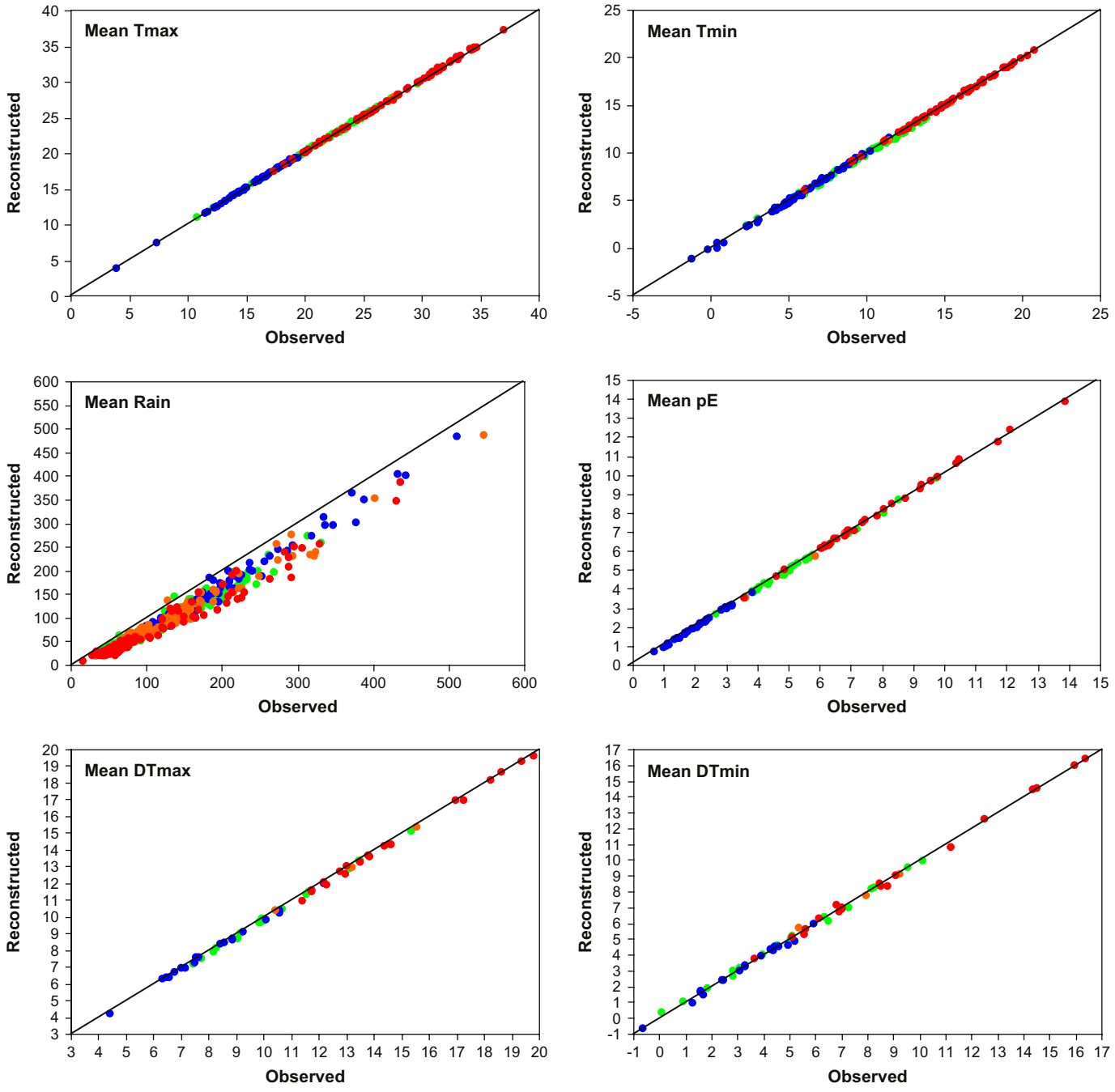

Fig. 5. Scatter plot of the reconstructed versus observed mean of the series for the six predictands. On each graph, there is one point per station and per season, the total number of points per graph is the number of stations across the six regions times four. The line of perfect fit (the diagonal) is shown. The colour code refers to season: blue is winter, green is spring, red is summer and orange is autumn. Units are °C for temperatures and dew-point temperatures, mm for rainfall and mm day^{-1} for pan evaporation. (For interpretation of the references to colour in this figure legend, the reader is referred to the web version of this article.)

T_{min} and dT_{max} than for pan evaporation and dT_{min}. For rainfall, correlations are by far the lowest, although due to the very large sample considered (about 4500 days); all these correlations are significant at least at the 95% level (based on rain occurrences only in the case of rainfall), indicating some level of skill. For most variables there is a marked seasonal cycle in skill, consistent across all regions: i.e. the analogue approach is particularly successful in autumn and spring for temperature predictands T_{max} and T_{min} (nearly reaching a correlation of 0.9 for T_{max} in autumn in several regions) and for pan evaporation (albeit with lower values). For rainfall, although correlations are low across all seasons, they peak in winter (between 0.3 and 0.4). For dew-point, seasonal variations of the results are less marked and not consistent across regions. Finally, there seems to be a high consistency in the performance of the SDMs across the six regions considered. Overall no particular region stands out as a climatic entity where the SDM skill in reproducing day-to-day variability is consistently lower or higher across all variables and seasons. The fact that the model was assumed to be applicable in all the extra-tropical part of the Australian continent where the climate is driven by synoptic disturbances is vindicated by these results.

The ability of the modelled series to reproduce year-to-year variability is also important in a climate change context. It is evaluated by computing the Pearson correlation between seasonal

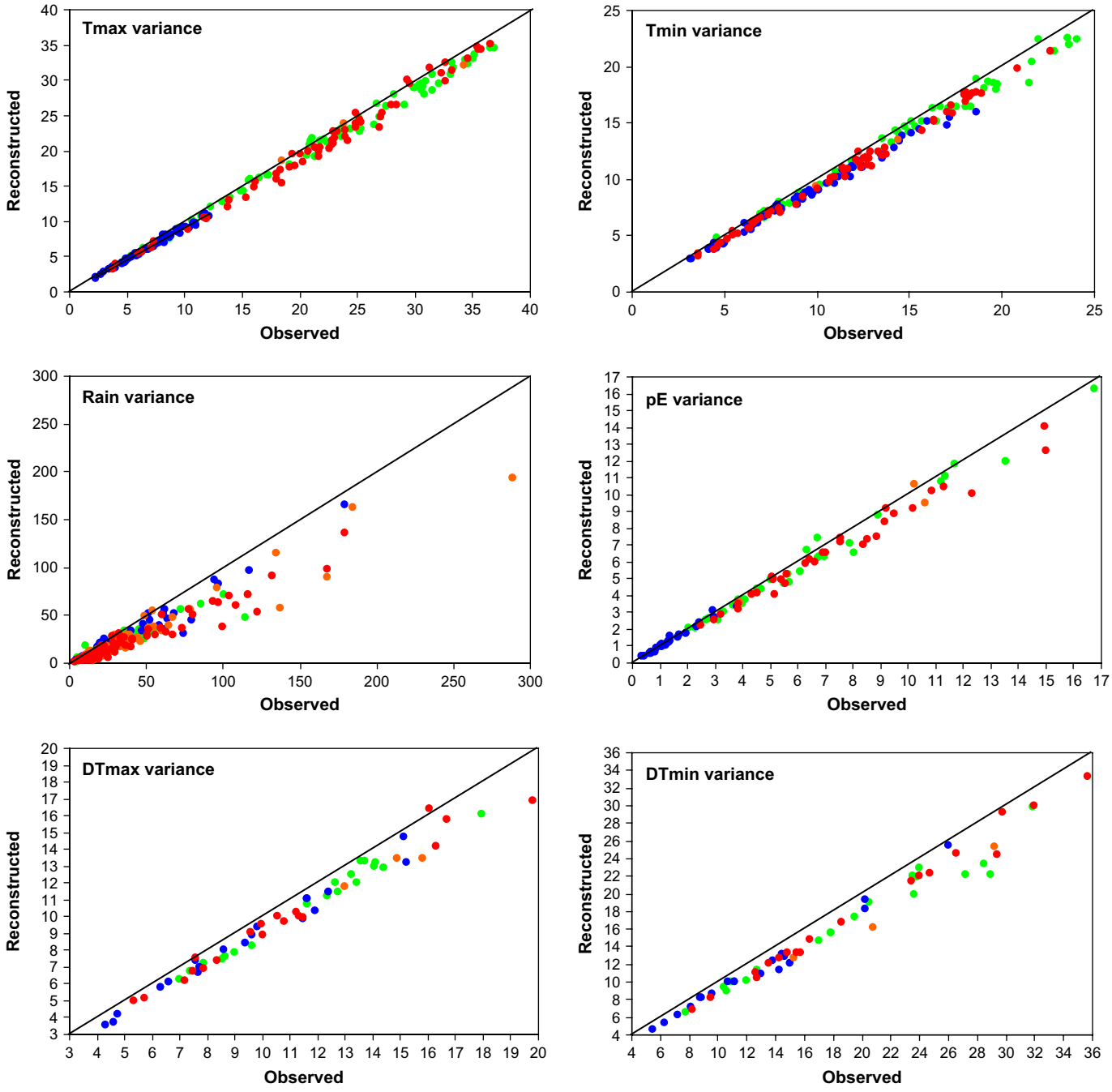

Fig. 6. As per Fig. 5 but for standard deviations (units as for the means).

means of the observed and reconstructed series (Fig. 9) in the same way as daily variability. The length of observed record is 1958–2003 for all predictands apart for pan evaporation which is 1975–2003. The percentage of observed inter-annual range (i.e. the difference between the highest and lowest seasonal totals in the observed record) reproduced by the reconstructed series is also evaluated (Fig. 10). Overall, the SDMs show slightly better correlation on an inter-annual time-scale compared to a daily time-scale, but results are very consistent between the two time scales. The lowest correlation values are obtained for rainfall (albeit much improved compared to the daily time-scale) and highest for temperature. The seasonal variations of the results grossly resemble what was noted on the daily time-scale, but if anything is slightly less obvious: either differences are smaller or consistency across regions is not as strong. For rainfall, the model is most able to reproduce inter-annual variability in winter (as that was the case for daily variability) and in autumn for dew-point (that was also the case for daily variability). Although, the correlations suggest that the technique is able to capture most of the inter-annual variability, it appears to reproduce only a fraction of the inter-annual range (Fig. 10). Results are particularly low for pan evaporation (below 50% in most instances) and dT_{min}. For T_{max}, the percentage of reproduced variance is low in winter (30–60%) but mostly above 50% in other seasons. These seasonal differences are less pronounced for T_{min}. For rainfall (note the different y-axis scale compared to the other variables), the percentage of observed variance reproduced is much higher, mostly between 60% and 100%, but exceeds 100% in several instances. Again that is a flow-on effect of the correction factors applied to the reconstructed series, as earlier results showed that without correction, the reproduced

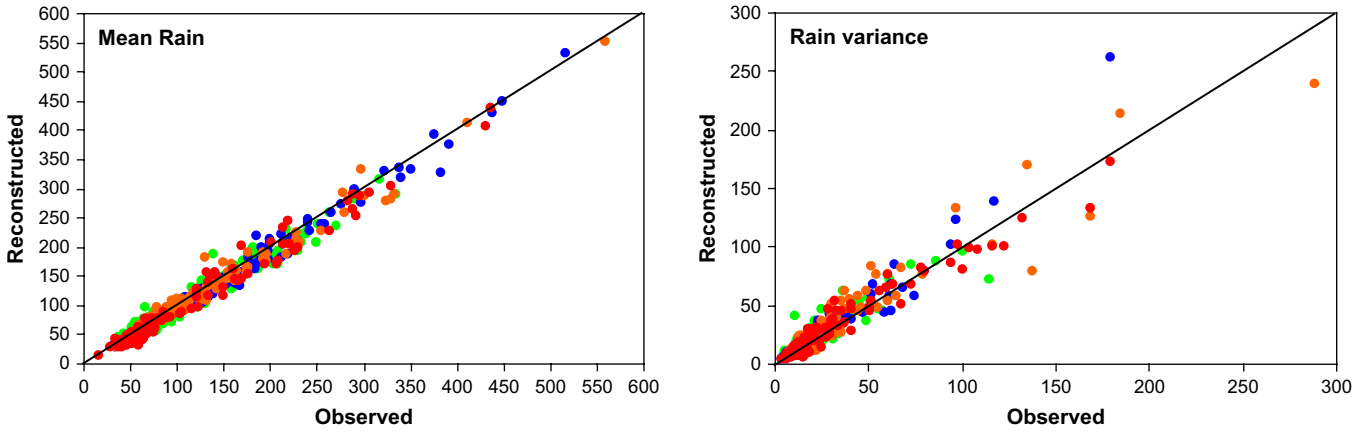

Fig. 7. Scatter plot of the reconstructed versus observed mean (left) and variance (right) for rainfall, with an inflation factor applied to the reconstructed series (see main text for details). Unit is mm.

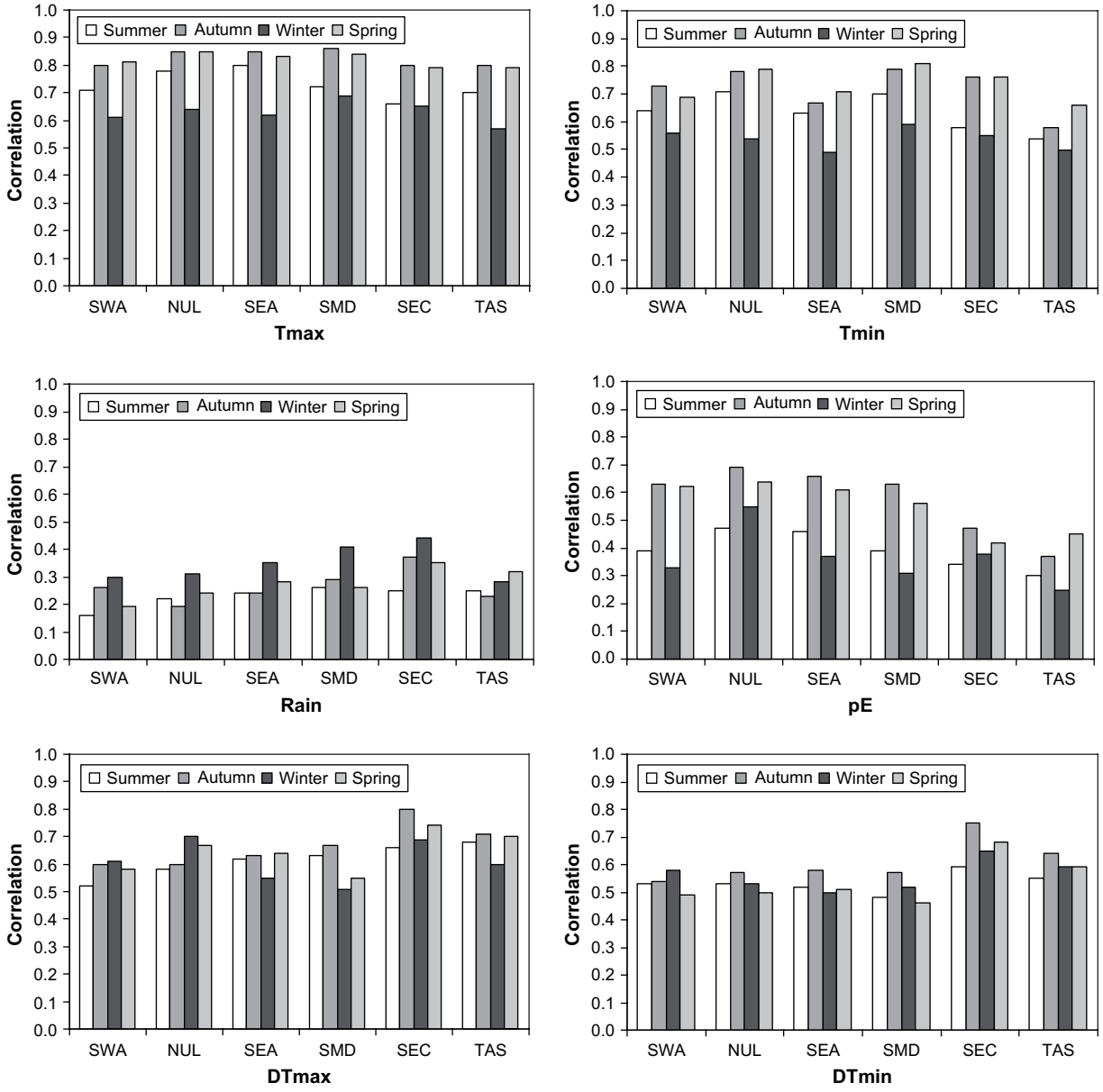

Fig. 8. Correlation between daily observed and reconstructed series specified by season (different coloured bars) and region (names on the *x*-axis) for the six predictands considered (names in the bottom left corner). Each correlation is an average across all the stations available in a particular region. (For interpretation of the references to colour in this figure legend, the reader is referred to the web version of this article.)

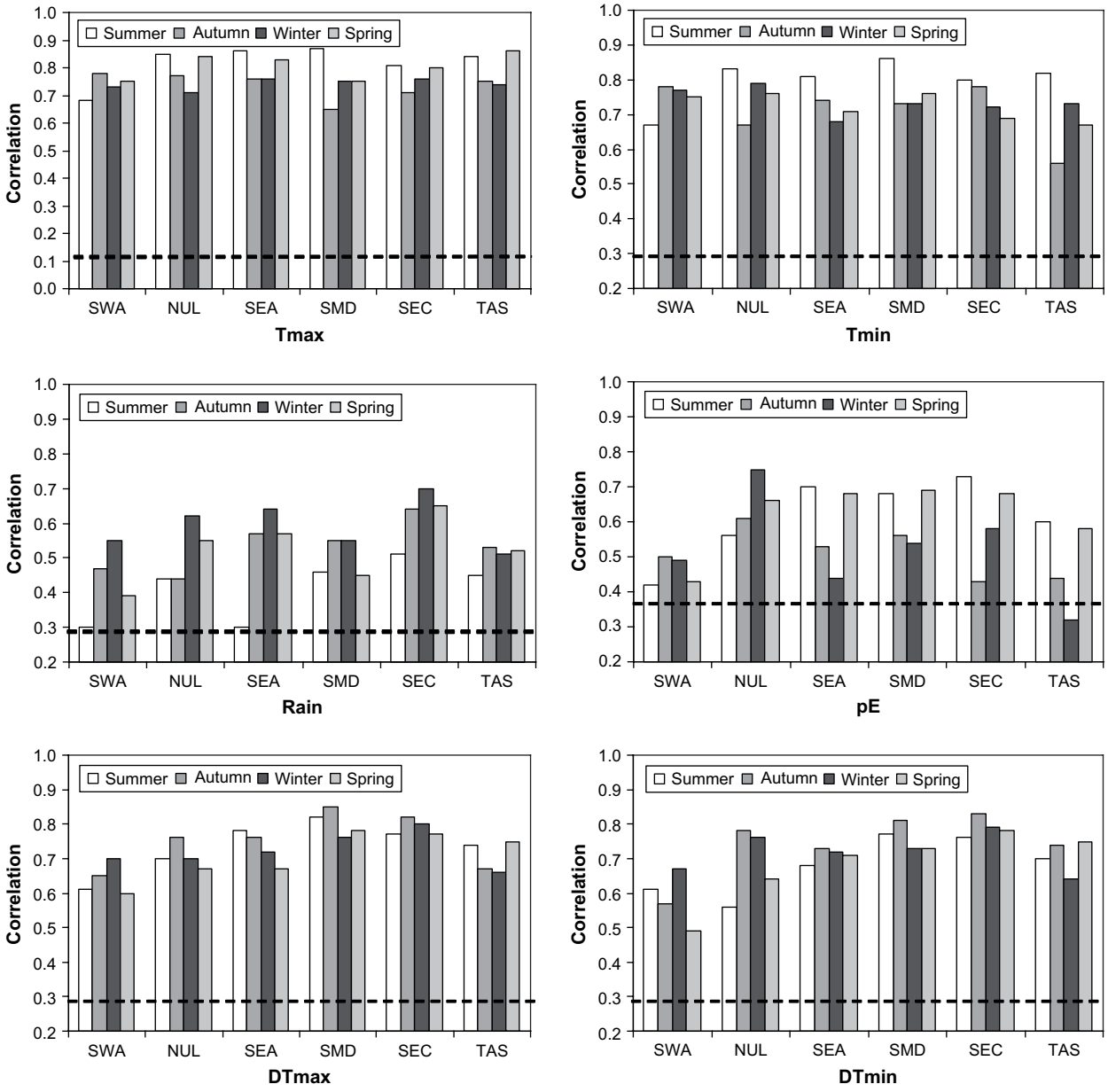

Fig. 9. As per Fig. 8 but for seasonal means. In addition, the dash line indicated the 95% confidence level for these correlations.

inter-annual variability was underestimated for rainfall as well (Timbal, 2004).

Finally, an important validation step is to analyse the ability of the SDMs to capture observed long-term trends. This provides confirmation that the large-scale predictors capture the forcing that explains local trends and hence gives confidence in the ability of the SDM to reproduce realistic local changes driven by large-scale changes in future projections. Linear trends were fitted to all stations and regional averages are compared with similar trends from reconstructed series calculated for the length of the series: 1958–2003 for all predictands apart from pan evaporation (1975–2003) (Fig. 11). Each point on these graphs is a regional average of the available HQ stations, thus 24 points (four seasons and the six regions) are shown. On each graph, the line of best fit (constrained to intercept with 0) between the observed and reconstructed series is shown (solid line) as well as the slope of the relationship and the correlation between the two variables (indicated in the bottom right corner of each graph). In general, the reconstructed series exhibit trends of a magnitude strongly related to the observed trends: the correlation varies between percentage 0.87 for rainfall and 0.46 for dT_{min}, suggesting that the SDMs have skill in reproducing the observed trends. However, the slope of these relationships is constantly less than one (between 0.14 and 0.78), pointing to an underestimation of the observed trend, which is of concern in regard to the ability of the SDM to reproduce the magnitude of the future changes.

Since the reconstructed series reproduced only part of the inter-annual range it is expected that this would affect the linear trend fitted on the reconstructed series. The impact of this underestimation of the inter-annual range can be shown by plotting the same graph for the *normalised linear trend* of the reconstructed series where the trend is divided by the ratio of reproduced inter-annual range (from Fig. 10) and shown as crosses in Fig. 11. Although the correlations between series (indicated in the top left corners of each graph) remain by and large unchanged, the slope of the relationship (dashed line) in most cases is much closer to one (usually around 0.88). This is a major improvement, except for rainfall (but again, rainfall did not have a marked underestimation of the inter-annual range due to the correction factor applied) and

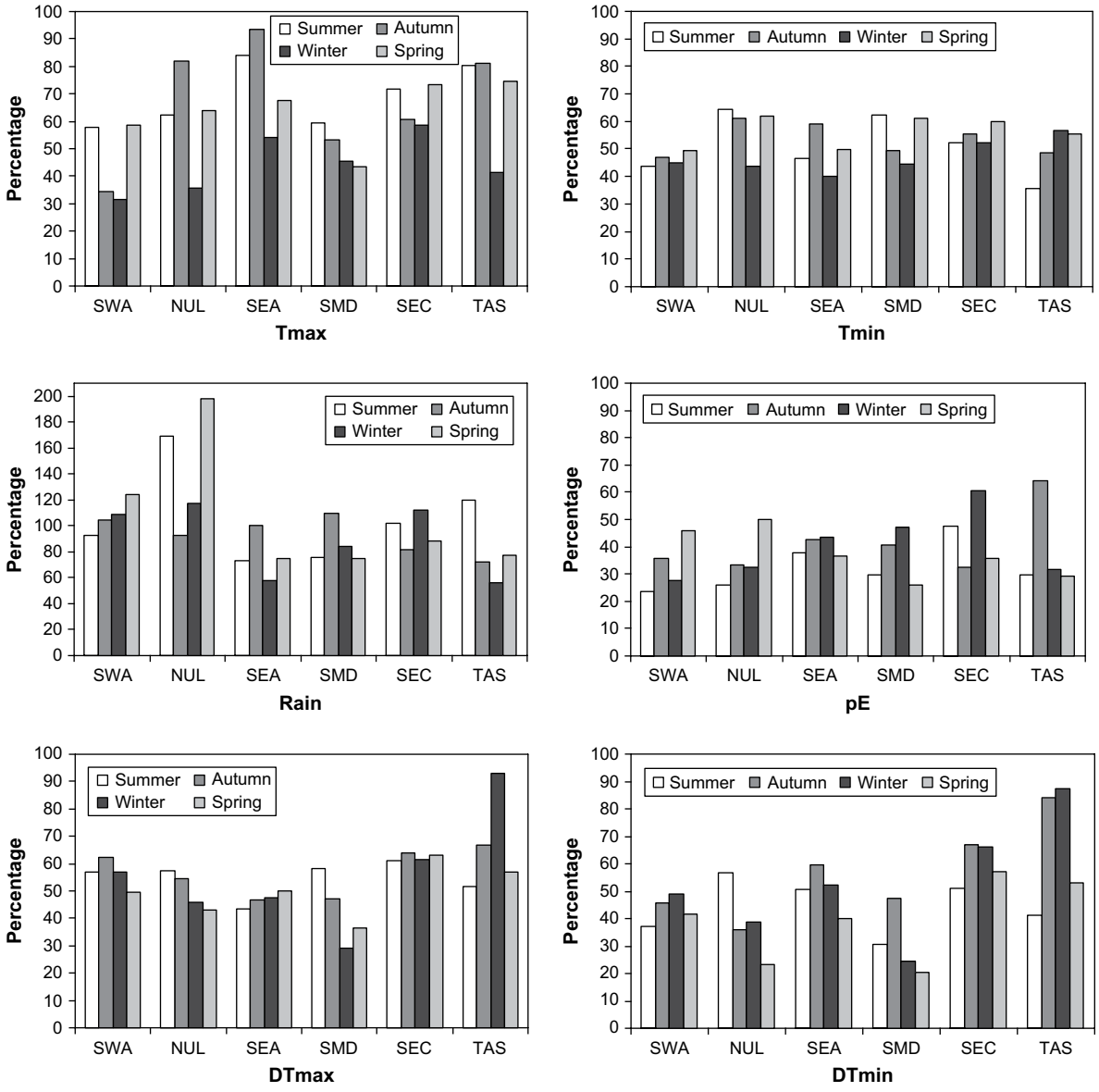

Fig. 10. As per Fig. 8 but for the percentage of the observed inter-annual variance reproduced by the reconstructed series.

dT_{min}, for which the slope remains very low. This latest finding enhances the confidence in the model's ability to reproduce future climate changes at the local scale, as it is able to do so for the current on-going climate changes once the underestimation of the variance on inter-annual scale is factored in. This is an important caveat and should be noted by users of the downscaled projections as the currently available projections do not factor in this correction. The result for dT_{min} however, casts some doubt on the validity of future projections for this variable.

Following the evaluation of the SDM's skill in reproducing the most important characteristics of the observed local predictands such as mean, variance, day-to-day and inter-annual variability as well as long-term trends, the optimised SDMs were found useful and capable of reproducing valuable information at the local scale. Optimised SDMs were then applied without further adjustment to the CMIP3 climate models described earlier. It is worth noting that the search for analogues is performed on normalised anomalies of the predictor fields. In the case of climate model simulations, normalised anomalies are calculated for the simulation of the 20th century, in effect removing model biases in the mean and variance reproduction of predictor fields. The model mean climatology is then used as a baseline to calculate anomalies for the predictors in future projections. This methodology assumes that the same model biases are affecting future projections and is commonly used in climate change science. Implicitly, this methodology corrects model biases both in the mean state and in daily variability and therefore the traditional evaluation of the GCM performances in reproducing surface predictands (as used in the Climate Change in Australia report (CSIRO and BoM, 2007)) is not relevant here. However, a careful evaluation of the suitability of downscaled models for any impact study should be performed by any users, using the local predictands of interest generated by downscaling GCMs' simulation of the 20th century (20C3M). Results were gathered in a large dataset and the tool used to explore this dataset is now presented.

5. The software structure

The GUI to disseminate the downscale projections has been constructed using three static HTML pages using Java script (Fig. 12). Additional pages are generated dynamically using Perl. These output the data as it is extracted from the datasets in response to user inputs. The last component of the GUI is an

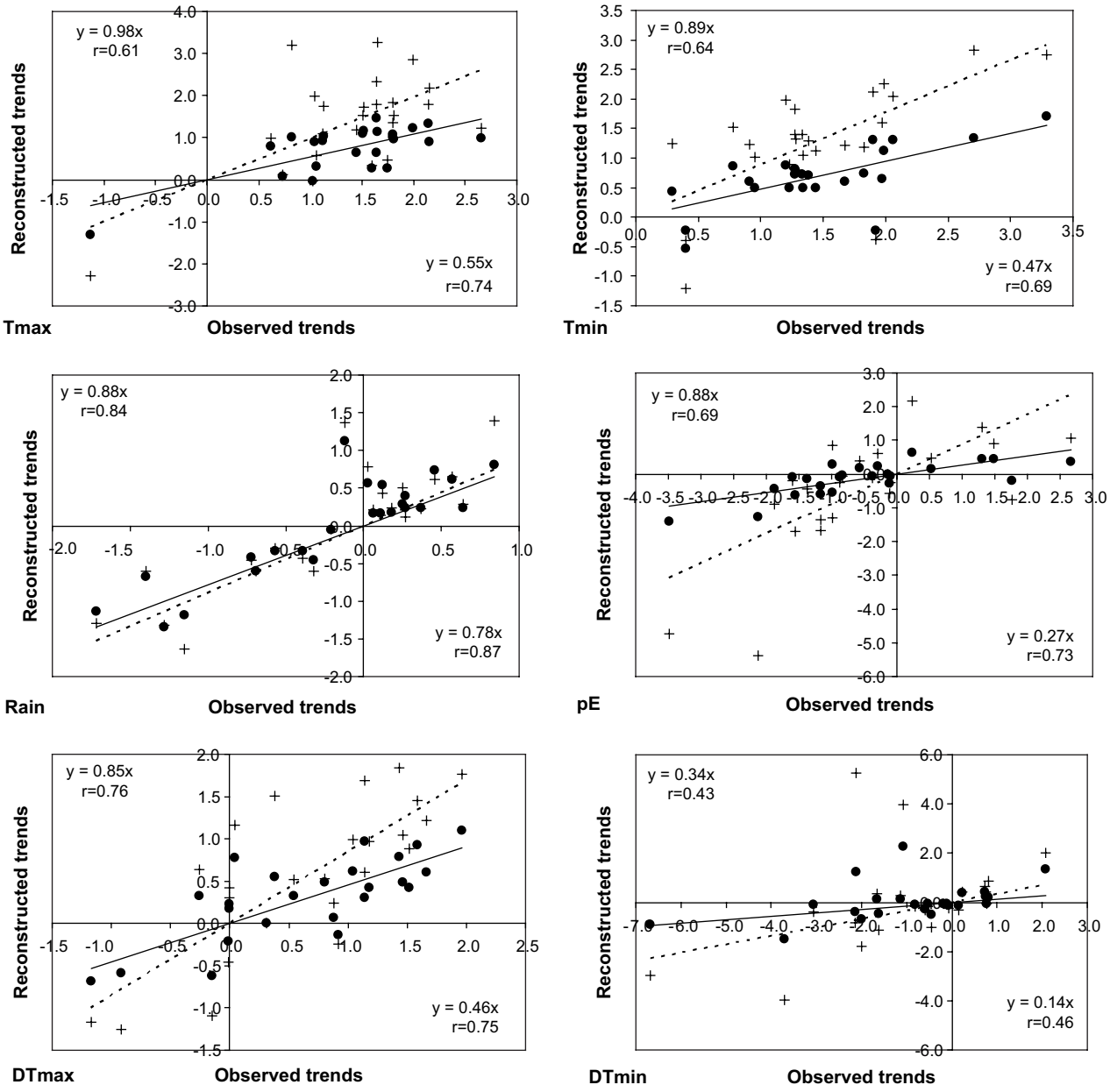

Fig. 11. Scatter plot of the reconstructed versus observed linear trends fitted on the length of the longest possible record for the six predictands (dots) as well as for the normalised reconstructed trends (+ signs). For each series, there is one point per seasons and per regional average for all existing stations in that region. The total number of point per series is 24: six regions times four seasons. The line of best fit is shown by the full (dashed) line and its slope as well as the correlation between the two variables in the bottom right (top left) corner for the (normalised) reconstructed series.

Interactive Data Language (IDL©) script which starts the calculation of the SDM itself. The starting point of the GUI displays a large region around the Australian continent using MapData© powered by Google. It provides an option to choose the background between physical maps, satellite images or a combination of both (using buttons displayed at the top right). The user has a series of four steps to follow in order to carry out the downscaling process (they are illustrated in Fig. 13):

1. Select a predictand from the *Predictand* dropdown list (rainfall, T_{max}, T_{min}, pE, dT_{max} or dT_{min}) and select one of the austral calendar seasons from the *Season* dropdown list: summer, autumn, winter, spring (in Fig. 13, T_{max} and summer are chosen).
2. Choose the model(s) from the *Model* dropdown list (select an individual CMIP3 model or choose all available models) and a scenario from the *Scenario* dropdown list (either the 20th century simulation, providing daily data from 1961 to 2000, or future emission scenarios A2 and B1 for the 21st century, providing daily data for 20-year time slices: 2046–2065 for A2_50 and B1_50 and 2081–2100 for A2_100 and B1_100). In Fig. 13, A2_50 and all available models were chosen.
3. Select one of the six climate regions from the Australian map. This provides a higher resolution map of the region showing available stations with a mark within the rectangular area that can be selected individually by a click or as a whole group on the left. In Fig. 13, the SMD region was selected and the Mildura station already selected appears in the left station box while other stations within the SMD regions are still shown by a marker on the map.
4. Start the downscaling process by enabling the button *Run Downscaling*. In Fig. 13, the GUI is ready for the user to enable that button.

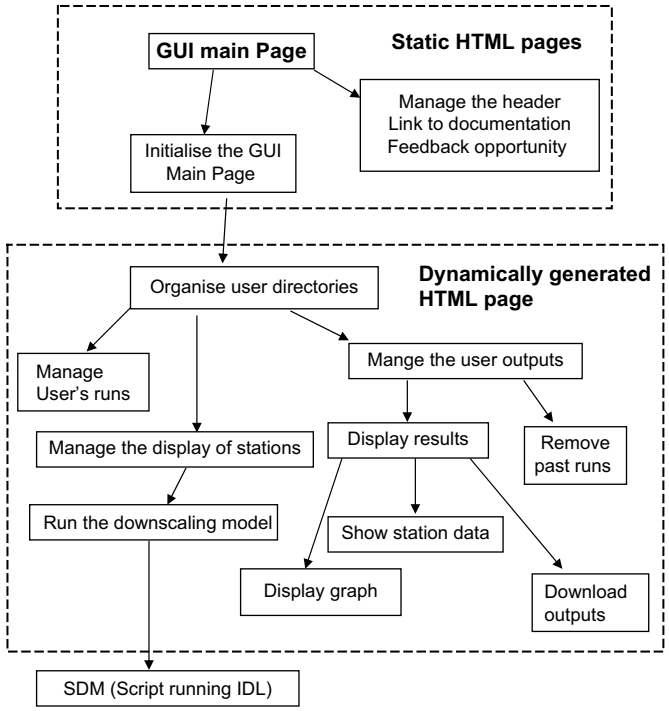

Fig. 12. Architecture of the graphical user interface used to access results from the BoM Statistical Downscaling Model.

Only a part of the entire SDM code is run on the fly to generate graphics and data output. It relies on intermediary files pre-calculated for all possible cases chosen with the GUI. These intermediary files are labelled *Change-Of-Date* (COD) files and contains the optimum analogue (i.e. a single best match) for any model day chosen amongst the 1958–2003 period in the NNR database (apart from pan evaporation where it is restricted to 1975–2003). This optimal analogue depends on all the parameters chosen in the GUI: the predictand, the season, the region and the individual synoptic situation produced by the CMIP3 GCM. Upon completion of the downscaling calculation, a table is generated and appears underneath the user interface containing information about the downscaled simulation just completed and the outputs available: one data file per station chosen and some graphical outputs. All files, graphics and underlying data can be downloaded by the user.

6. Downscaled projections: a case study

To illustrate the benefit of the tool and the usefulness of obtaining detailed point specific climate change projections, a case study was completed using the GUI. In this example, maximum daily temperatures in summer were sought for Mildura, which is an important regional centre in the northwest of Victoria in particular for agriculture (located within the SMD region). Additional case studies for both temperature and rainfall can be found in the Climate Change in Australia report (CSIRO and BoM, 2007).

The downscaling of all climate models provides a good estimate of the local PDF for T_{max} in summer in Mildura (Fig. 14, top left). The mean and variance from the downscaling of the GCMs encompass

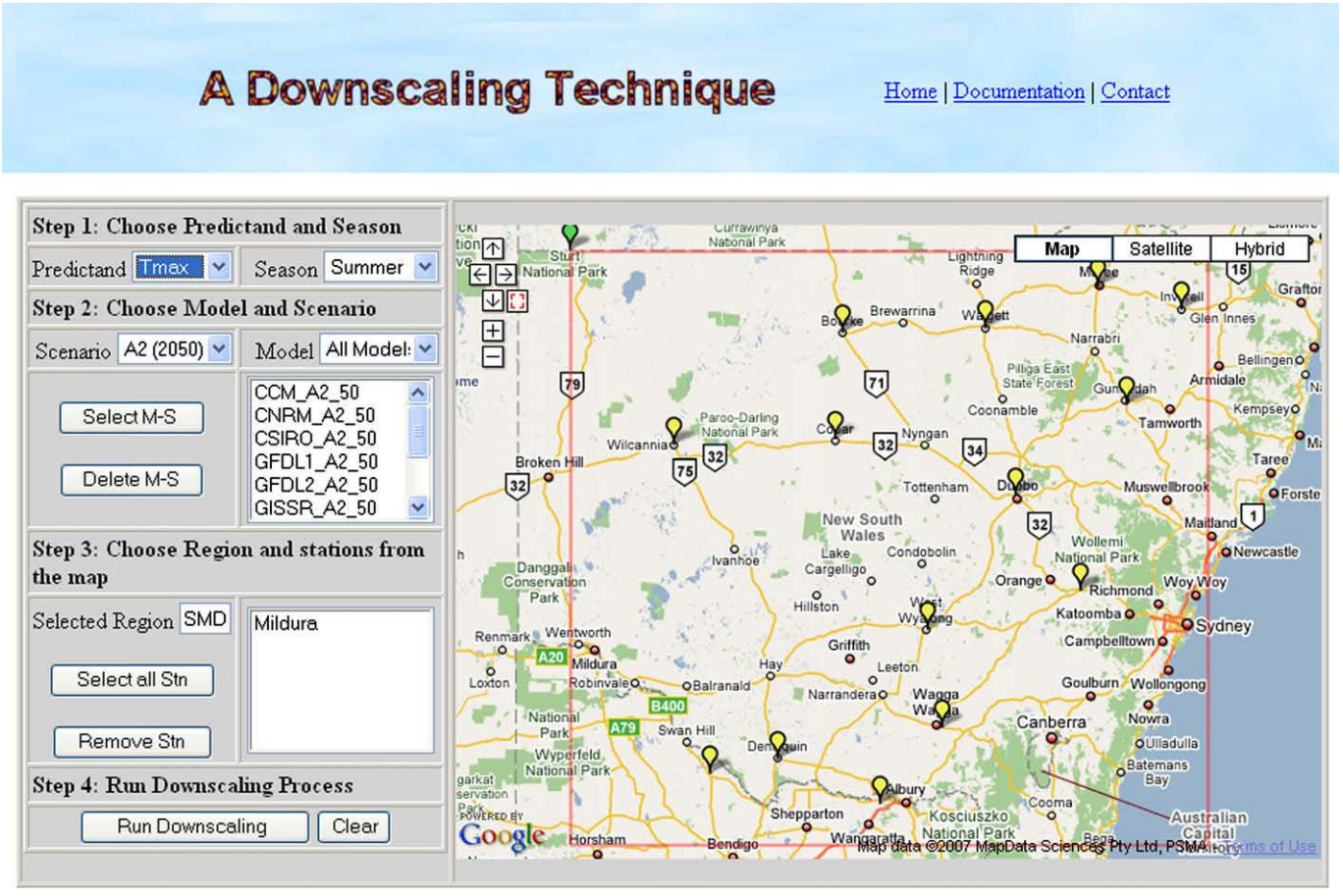

Fig. 13. View of the GUI once the user has selected a few options (see main text for details).

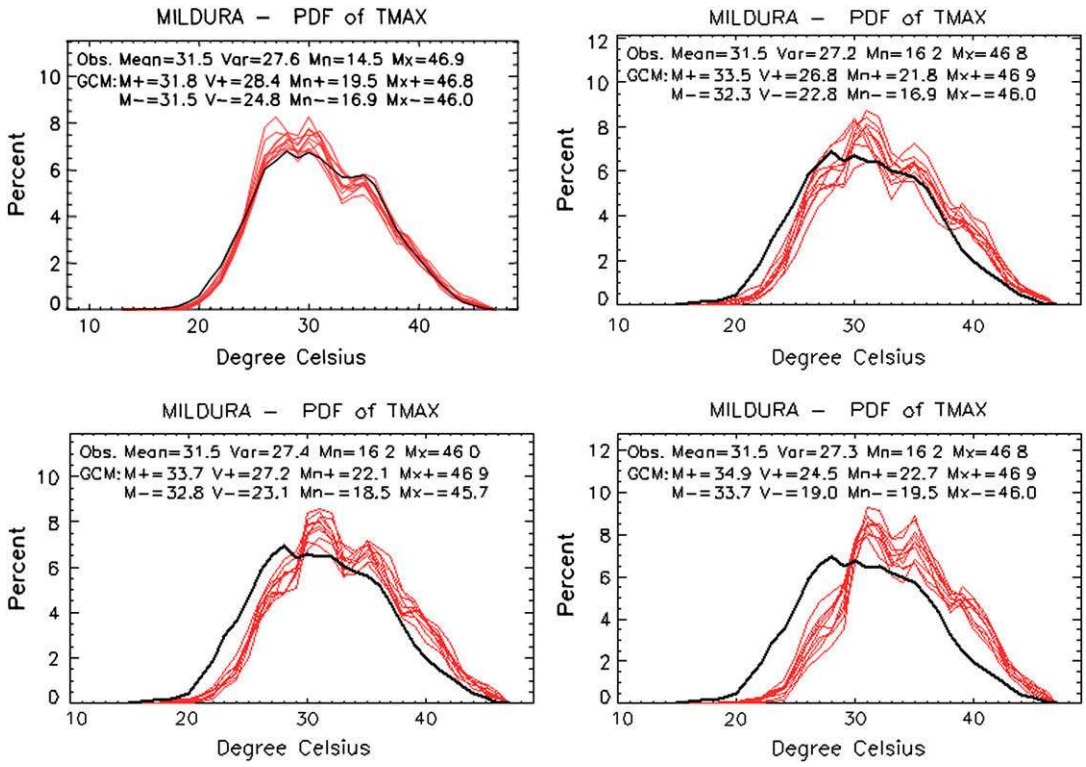

Fig. 14. Probability distribution functions of maximum temperature in summer in Mildura (Victoria, located in SMD) for the end of the 20th century (top left) and for the middle of the 21st century using emission scenario B1 (top right). Similar plots show the scenario A2 for the middle (bottom left) and the end of 21st century (bottom right). Observations are shown as a thick black line, and the downscaling of each of the 10 individual climate models from the CMIP3 database is shown as red lines. Mean, variance, maximum and minimum of the series are shown on the graphs as the top line with the range of the same statistics across the 10 downscaled models (note: for the mean the results are expressed as a difference from the observed mean). (For interpretation of the references to colour in this figure legend, the reader is referred to the web version of this article.)

the observed values (observation statistics are shown on the top line in each diagram, while the model range is given in the following two lines). It is worth noting that the particular shape of the PDF with a broad maximum around 28 °C and a secondary maximum around 35 °C is also captured. The transformation of the PDF under future projections is shown for 2050 for the B1 (Fig. 14, top right) and A2 scenarios (Fig. 14, bottom left) and for 2100 for the A2 scenario (Fig. 14, bottom right). With this order the graphs look at the details that local warming implies. It is worth noting that the observed PDFs are not strictly identical (nor are the statistics for the observations) in the case of the 20th century and for future projections. This is due to the different baselines: 1960–1999 for the 20th century and 1970–1989 for future projections.

One of the criticisms often made about downscaled climate change projections is that it is not possible to validate the underlying assumption that the statistical linkage remains valid in a warmer world (Hewitson and Crane, 2006). Although this point was partially answered during the model evaluation stage by showing that the SDMs were able to reproduce the observed trends. In this case study, it is possible to compare the point specific projections with direct model projections coming from the CMIP3 models for grid boxes surrounding Mildura (documented in the Climate Change in Australia report, CSIRO and BoM, 2007 and available on-line at http://www.climatechangeinaustralia.gov.au/). Although this comparison is not a perfect match as numbers are coming from very different methodologies but it provides an interesting overview of the consistency amongst these different projections.

For 2050, direct model projections suggest a range for high emission scenarios between 1 and 1.5 °C at the 10th percentile, 2 and 2.1 °C at the 50th percentile and 2.5–3 °C at the 90th percentile, and for low emission scenarios, between 0.6 and 1 °C at the 10th percentile, 1 and 1.5 °C at the 50th percentile and 2–2.5 °C at the 90th percentile. These values are comparable with the suggested warming of 1.3–2.2 °C shown here for the A2 scenario (a high emission scenario) and 0.8–2 °C for the B1 scenario (a low emission scenario). The range is not as large as with the direct model outputs but in that case the entire CMIP3 database (23 models) was used compared with only 10 models in our case study. And the low and high emission scenarios in the CSIRO and BoM (2007) projections are based on more than the single scenario (B1 or A2) used here.

In addition to the mean local warming and the changes of the PDF it is possible to take a closer look at the details of the local warming implies. For example, the length and duration of hot spells (number of consecutive days above a particular threshold) can be looked at. The downscaling of the climate models underestimates the hot spell duration (Fig. 15). For example the probability that hot spells above 36.7 °C last up to 8 days is observed to be 0.01 in Mildura, the same probability for downscaled model suggest a spell length between 5 and 7 days (left graph in Fig. 15) but the thresholds used (which depends on the mean and variance of the individual series) matches the observed threshold. Keeping these results in mind, future projections of hot spell duration show that much larger thresholds are used (due to the mean warming) but the probability of spell length is hardly changed. Also, there is a small hint toward more likely long spell as model curves are slightly more bunched toward the observed trend then they were in the current climate case, but that may not be significant as it is likely to be by less than a day apart for more extreme spells (right graph in Fig. 15). Of course, if the threshold used for the 20th century was kept, results would be very different as days above 36.7 °C are projected to be far more frequent (as implied by the PDFs in Fig. 14). Looking at hot spell duration using a threshold fitted to the new distribution implies that the population and the environment would have

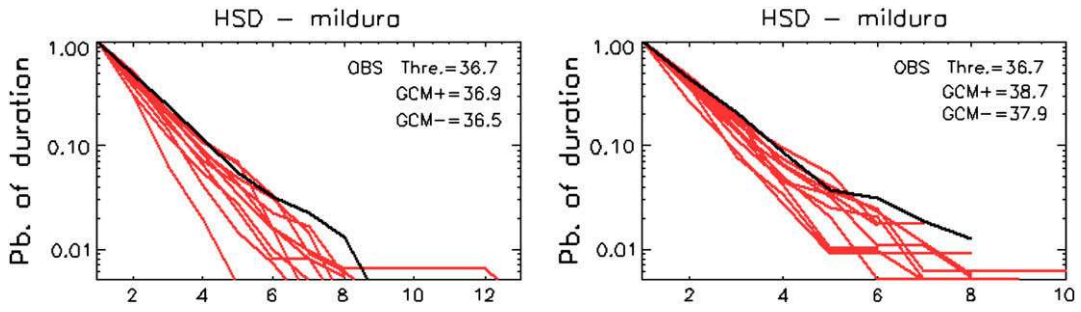

Fig. 15. Hot spell duration expressed as probability of exceedance above a certain threshold in number of days for T_{max} in summer in Mildura for the end of the 20th century (left) and for the middle of the 21st century using emission scenario A2 (right). Observations from 1960 to 1999 are shown as thick black line on the 20th century diagram and are repeated for the 21st century using 1970–1989 to provide a reference to compare downscaled model simulation for 2046–2065. The thresholds used depend on the mean and variance of the series and differs from observations to models and from the 20th century to the 21st century and are shown on the graphs.

adapted to the mean warming. However, as users can access ASCII files with the daily values used to construct the PDFs, they can perform additional analyses on extremes and decide on which thresholds to use. The graphs generated by the GUI (Figs. 14 and 15) serve to illustrate the main characteristics of the downscaled results and the possibility of generating many analyses, as the locally constructed daily series (in the 20th century climate) are highly realistic.

When dealing with extremes and using downscaled projections it is important to keep in mind that the statistical linkage established using the data is more likely to be robust for the middle of the distribution, for which there are more observations, than for the extremes which are not so extensively sampled. For example, since the SDM uses an analogue approach, it is not possible to get daily projected values that have not been observed before (e.g. new record temperatures). In the case study, the maximum value is tied to the past record in summer observed at Mildura during the 1958–2003 period: 46.9 °C. This explains why despite the mean warming (e.g. for A2_100, bottom right in Fig. 14), the upper tail of the distribution do not shift right with the rest of the distribution. This situation can be contrasted with what is happening for record low temperatures, shifting from 16.2 °C to between 19.5 and 22.7 °C, a massive increase of up to 6.5 °C by 2100 with the A2 scenario (compared to the lowest value observed between 1970 and 1989). Similar shifts might be a reasonable assumption for recording hot temperatures but it is not possible to infer this from the current set of results. Therefore, in the case of warm extremes, only the frequency of occurrences below the local record temperature would be meaningful for future projections.

7. Concluding remarks and future prospects

The application of the BoM statistical downscaling model, developed in earlier studies, has been generalized across half of the Australian continent. This method provides point specific climate change projections relevant for impact studies across the continent in locations where high-quality observations of the current climate are available. Individual SDMs were optimised using the high-quality BoM network of observations for temperature (daily extreme: T_{max} and T_{min}), rainfall, dew-point temperature (daily extreme: dT_{max} and dT_{min}) and pan evaporation. Stations were lumped into regional climate entities, six in total: five covering the southern part of the continent from the southwest of Western Australia to the east coast, and one for the island of Tasmania. Each individual SDM was optimised in two steps: first the optimal combination of predictors was determined and then additional parameters of the statistical model (size of the domain to choose the predictors, calendar window and method to calculate daily anomalies) were determined. In total, 144 individual SDMs were optimised: six predictands times six regions times four seasons.

This extensive work was possible due to the simplicity of the chosen downscaling method. The analogue approach used here is one of the simplest existing downscaling methods. Despite its simplicity which was paramount to be able to perform this work, this method has been shown to compare well with more advanced techniques (Zorita and von Storch, 1999). The simplicity, flexibility and robustness of the technique were important to ensure that a single technique could be used across a range of variables and several climatic regions.

A careful evaluation of the skill of the SDM was carried out on different time scales: daily, inter-annual and long-term trends. The technique was found to reproduce the main characteristics of the PDFs of local observed variables. In particular the technique was found to be unbiased and it was able to reproduce the local means. However, like most statistical downscaling techniques, it was shown that the analogue approach does not fully reproduce the observed variances of the series. That limitation was found to exist across all variables with a varying degree of severity. This drawback was found to be particularly important for rainfall; due to the non-normal distribution of daily rainfall, the reduction of variance leads to an underestimation of the mean (Timbal et al., 2006). It was therefore decided to introduce a correction factor for rainfall applied to the reconstructed series and based on the local observed climate. It was done so as to reduce the underestimation of the variance and reproduce an unbiased mean. This correction was kept to a very simple level and is unchanged across all rainfall stations and seasons, in order to minimise the risk of over-fitting based on the current climate.

It was shown that the technique overall was skilful at reproducing the observed PDFs for the right reasons. The daily variability is well reproduced, as captured by the day-to-day correlation between the observed and reconstructed series. In addition, the technique has skill in capturing inter-annual variability as well as long-term observed climatic trends.

It is notable that although the analogue approach is least skilful in terms of correlation (on both daily and inter-annual time-scale), for rainfall, it gives the most reliable reproduction of long-term trends of all predictands. This suggests that day-to-day variability of rainfall amount is largely affected by local effects not captured by large-scale variables. The large-scale variability and long-term trends, which remove a lot of this small temporal scale variability, is well tied to large-scale factors.

By contrast, the technique, while is extremely skilful in reproducing temperature series on daily and inter-annual time scales, appears to consistently underestimate (by a factor of two) observed long-term warming. It was found that this underestimation is by and large due to the underestimation of the variance by the reconstructed series, leading to an underestimation of the magnitude of the trend.

For newly developed moisture variables, the analogue technique performed relatively consistently with skill displayed across

all statistics within the range of the two extremes provided by temperature and rainfall. It was noted however, that for dT_{min}, the technique does not appear to reproduce much of the observed long-term trend, thus casting doubt on the ability of large-scale predictors to explain local trends for this variable and hence suggesting that the method may not be able to provide meaningful downscaled projections.

Up to a point, the tendency for the SDMs to reproduce only part of the observed long-term trend cast doubts on the technique's ability to realistically downscale future projections of global warming. However, some of these doubts were alleviated when, as a case study, future projection for T_{max} in Mildura (Victoria), in the south-east of Australia were presented in detail. Projected local warming using the downscaling approach appears comparable to published projection for the area surrounding this location (CSIRO and BoM, 2007). This case study illustrates the outputs available using a newly developed graphical user interface to disseminate local downscaled climate change projections.

This is a landmark project, offering downscaled climate change projections across a large part of the Australian continent. It is worth noting that currently, downscaled predictand series are constructed independently from one variable to another. This is possibly a limitation for impact studies that require several predictands (i.e. rainfall and temperature), although this possible issue was not investigated as part of this study. Further on-going developments are underway to maximise the benefits from this work. Currently the technique is being tested for the tropical part of the Australian continent in a bid to develop a nation-wide facility. However, the adaptation of a synoptically driven technique to tropical areas is not straightforward. Results presented here show that the technique is less skilful during hot weather (in summer) in particular for rainfall in northernmost regions of Australia. Previous attempts to downscale rainfall for tropical regions show the importance of using direct model outputs, such as rainfall, in order to reproduce the local rainfall (Robertson et al., 2004).

Additional planned developments concern (1) web access to the GUI and (2) providing gridded projections. Currently the GUI is only available internally within the BoM, and is used by regional climate services to provide tailored climate change projections upon request. The model is currently being ported on a national computing facility (the Australian Partnership for Advanced Computing, APAC) to provide a wider access for the research community. Furthermore, plans to provide outputs directly to the general public, as part of a larger climate projection on-line a central portal providing access to observe climate data and future projections generated by different methods (OzClim or the BoM SDM) are being investigated. In addition, the BoM has developed daily high resolution (0.05 by 0.05 degree) gridded data for rainfall and temperature (Jones et al., 2007). This is an interesting development that could be used in the current framework to provided downscaled climate change projections on the same grid scale.

Acknowledgements

The development of the Bureau of Meteorology (BoM) statistical downscaling technique has long been supported by the Department of Climate Change (DCC). The latest development of the graphical user interface was undertaken as part of the Australian Climate Change Science Program (ACCSP) supported by the DCC. The extension of the technique to moisture variables was supported in part by the ACCSP and in part by the South-Eastern Australian Climate Initiative (SEACI). The predictand databases were obtained from the National Climate Centre (NCC) of the BoM. We acknowledge the international modelling groups for providing their data for analysis, the Program for Climate Model Diagnosis and Intercomparison (PCMDI) for collecting and archiving the model data, the JSC/CLIVAR Working Group on Coupled Modelling (WGCM) and their Coupled Model Intercomparison Project (CMIP) and Climate Simulation Panel for organizing the model data analysis activity, and the IPCC WG1 TSU for technical support. The IPCC Data Archive at Lawrence Livermore National Laboratory is supported by the Office of Science, U.S. Department of Energy. Thanks are due to Aurel Moise and Lawson Hanson from the BoM for transferring the CMIP3 database to Australia. The help of Bradley Murphy from NCC in setting the surface moisture dataset and initiating some of the early work on these variables is acknowledged. The authors wish to thank G. de Hoedt, R. Colman and three anonymous reviewers for their constructive criticisms on earlier versions of this article.

References

Bannayan, M., Hoogenboom, G., 2008. Weather analogue: a tool for real-time prediction of daily weather data realizations based on a modified k-nearest neighbor approach. Environ. Model. Software 23 (6), 703–713.

Burton, A., Kilsby, C, Fowler, H., Cowpertwait, P., O'Connell, P., 2008. RainSim: a spatial–temporal stochastic rainfall modelling system. Environ. Model. Software 23 (12), 1356–1369.

Charles, S., Bates, B., Whetton, P., Hughes, J., 1999. Validation of downscaling models for changed climate conditions: case study of southwestern Australia. Clim. Res. 12, 1–14.

Charles, S., Bates, B., Viney, N., 2003. Linking atmospheric circulation to daily rainfall patterns across the Murrumbidgee River Basin. Water Sci. Technol. 48 (7), 233–240.

Christensen, J., Hewitson, B., Busuioc, A., Chen, A., Gao, X., Jones, R., Kolli, R., Kwon, W.-T., Magaña Rueda, V., Mearns, L., Meñendez, C., Raisanen, J., Rinke, A., Sarr, A., Whetton, P., 2007. Climate change 2007: the physical science basis. Contribution of Working Group I to the Fourth Assessment Report of the Intergovernmental Panel on Climate Change: Regional Climate Projections. Cambridge University Press, Cambridge, United Kingdom and New York, NY (Chapter 11).

CSIRO, Bureau of Meteorology, 2007. Climate Change in Australia, Technical Report. Australian Greenhouse Office. www.climatechangeinaustralia.gov.au, 148 pp.

Drosdowsky, W., 1993. An analysis of Australian seasonal rainfall anomalies: 1950–1987. I: spatial patterns. Int. J. Climatol. 13, 1–30.

Hessami, M., Gachon, P., Ouarda, T., St-Hilaire, A., 2008. Automated regression-based statistical downscaling tool. Environ. Model. Software 23 (6), 813–834.

Hewitson, B., Crane, R., 2006. Consensus between GCM climate change projections with empirical downscaling: precipitation downscaling over South Africa. Int. J. Climatol. 26, 1315–1337.

Jones, D., Wang, W., Fawcett, R., 2007. Climate Data for the Australian Water Availability Project, Final Milestone Report. Bureau of Meteorology.

Jovanovic, B., Jones, D., Collins, D., 2008. A high quality monthly pan evaporation dataset for Australia. Clim. Change published online.

Kalnay, E., Kanamitsu, M., Kistler, R., Collins, W., Deaven, D., Derber, J., Gandin, L., Iredell, M., Saha, S., White, G., Woollen, J., Zhu, Y., Chelliah, M., Ebisuzaki, W., Higgins, W., Janowiak, J., Mo, K., Ropelewski, C., Wang, J., Leetma, A., Reynolds, R., Jenne, R., Joseph, D., 1996. The NCEP/NCAR 40-year reanalysis project. Bull. Am. Meteorol. Soc. 77, 437–471.

Kilsby, C., Jones, P., Burton, A., Ford, A., Fowler, H., Harpham, C., James, P., Smith, A., Wilby, R., 2007. A daily weather generator for use in climate change studies. Environ. Model. Software 22 (12), 1705–1719.

Lavery, B., Kariko, A., Nicholls, N., 1992. A historical rainfall data set for Australia. Aust. Meteorol. Mag. 40, 33–39.

Lavery, B., Joung, G., Nicholls, N., 1997. An extended high-quality historical rainfall dataset for Australia. Aust. Meteorol. Mag. 46, 27–38.

Lorenz, E., 1969. Atmospheric predictability as revealed by naturally occurring analogues. J. Atmos. Sci. 26, 636–646.

Lucas, C., 2006. A high-quality humidity database for Australia. In: Proceedings of the seventeenth Australia New Zealand Climate Forum, Canberra, Australia, p. 35.

Ricketts, J., Page, C., 2007. A web based version of OzClim for exploring climate change impacts and risks in the Australian region. In: MODSIM07 Proceedings, pp. 560–566.

Robertson, A., Kirshner, S., Smyth, P., 2004. Downscaling of daily rainfall occurrence over Northeast Brazil using a hidden Markov model. J. Clim. 17, 4407–4424.

Solomon, S., Qin, D., Manning, M., Chen, Z., Marquis, M., Averyt, K., Tignor, M., Miller, H.L. (Eds.), 2007. Climate Change 2007: the Physical Science Basis. Contribution of Working Group I to the Fourth Assessment Report of the Intergovernmental Panel on Climate Change, Chap. IPCC, 2007: Summary for Policymakers. Cambridge University Press, Cambridge, United Kingdom and New York, NY.

Solymosi, N., Kern, A., Maroti-Agots, A., Horvath, L., Erdelyi, K., 2008. TETYN: an easy to use tool for extracting climatic parameters from Tyndall data sets. Environ. Model. Software 23 (7), 948–949.

Timbal, B., McAvaney, B., 2001. An analogue-based method to downscale surface air temperature: application for Australia. Clim. Dyn. 17, 947–963.

Timbal, B., Dufour, A., McAvaney, B., 2003. An estimate of future climate change for Western France using a statistical downscaling technique. Clim. Dyn 20, 807–823.
Timbal, B., 2004. Southwest Australia past and future rainfall trends. Clim. Res. 26, 233–249.
Timbal, B., Arblaster, J., Power, S., 2006. Attribution of the late 20th century rainfall decline in Southwest Australia. J. Clim. 19 (10), 2046–2062.
Timbal, B., 2006a. Statistical downscaling in BMRC. In: Power, S., Pearce, K. (Eds.), Climate Change Research in the Bureau of Meteorology, pp. 68–72.
Timbal, B., 2006b. Statistical downscaling – an important part of ACCESS. In: Hollis, A. (Ed.), The Australian Community Climate and Earth System Simulator (ACCESS) – Challenge and Opportunities, pp. 123–126.
Timbal, B., Jones, D., 2008. Future projections of winter rainfall in southeast Australia using a statistical downscaling technique. Clim. Change 86, 165–187.
Trewin, B., 2001. The development of a high-quality daily temperature data set for Australia. In: Albuquerque, N.M. (Ed.), 11th Symposium on Meteorological Observations and Instrumentation, pp. 279–284.
Uppala, S., Kallberg, P., Simmons, A., Andrae, U., da Costa Bechtold, V., Fiorino, M., Gibson, J., Haseler, J., Hernandez, A., Kelly, G., Li, X., Onogi, K., Saarinen, S., Sokka, N., Allan, R., Andersson, E., Arpe, K., Balmaseda, M., Beljaars, A., van de Berg, L., Bidlot, J., Bormann, N., Caires, S., Chevallier, F., Dethof, A., Dragosavac, M., Fisher, M., Fuentes, M., Hagemann, S., Holm, E., Hoskins, B., Isaksen, L., Janssen, P., Jenne, R., McNally, A., Mahfouf, J.-F., Morcrette, J.-J., Rayner, N., Saunders, R., Simon, P., Sterl, A., Trenberth, K., Untch, A., Vasiljevic, D., Viterbo, P., Woollen, J., 2005. The era-40 re-analysis. Q. J. R. Meteorol. Soc. 131, 2961–3012.
Van Den Dool, H., 1994. Searching for analogues, how long must we wait? Tellus 46A, 314–324.
Von Storch, H., 1999. On the use of "Inflation" in statistical downscaling. J. Clim. 12, 3505–3506.
Wilby, R., Dawson, C., Barrow, E., 2002. SDSM – a decision support tool for the assessment of regional climate change impacts. Environ. Model. Software 17, 145–157.
Wilby, R., Charles, S., Zorita, E., Timbal, B., Whetton, P., Mearns, L., 2004. Guidelines for Use of Climate Scenarios Developed from Statistical Downscaling Methods, Published online, supporting material to the IPCC, 27 pp.
Zorita, E., von Storch, H., 1999. The analog method as a simple statistical downscaling technique: comparison with more complicated methods. J. Clim. 12, 2474–2489.